

# Stratospheric Flow and Solar Variability

By  
Bruce C. Macdonald

Department of Atmospheric Science  
Colorado State University  
Fort Collins, Colorado

This report was prepared with support from US Atomic Energy Commission  
under Grant No. AT(11-1)-1340.  
Principal investigator: E.R. Reiter  
April 1974

C00-1340-38

**Colorado  
State  
University**

**Department of  
Atmospheric Science**

Paper No. 223



STRATOSPHERIC FLOW AND SOLAR VARIABILITY

By

BRUCE C. MACDONALD

This report was prepared with support from  
U. S. Atomic Energy Commission  
Under Grant No. AT(11-1)-1340  
Principal Investigator: E. R. Reiter

Department of Atmospheric Science  
Colorado State University  
Fort Collins, Colorado

April, 1974

Atmospheric Science Paper No. 223



## ABSTRACT

### STRATOSPHERIC FLOW AND SOLAR VARIABILITY

A brief summary of recent research relating solar variability to weather elements on earth is presented. A response of stratospheric flow associated with the polar night vortex to this variability is determined beginning three to five days after the occurrence of a geomagnetic storm. The contour gradient at the 10 millibar surface near the edge of this vortex steepens, and the flow near the edge becomes more meridional. Warmings detected at this level tend to propagate downward. The reaction of the polar vortex flow seems to be most marked when the flow is nearly unstable. Some mechanisms presented by other workers in this field as well as the implications of these findings are discussed.

Bruce C. Macdonald  
Department of Atmospheric Science  
Colorado State University  
Fort Collins, Colorado 80521  
April, 1974



## ACKNOWLEDGEMENTS

The author wishes to express deep gratitude to Professor Elmar R. Reiter for his advice, encouragement, and constructive criticism both in the preparation of this thesis and throughout the author's graduate career. The kind assistance of Professor Bernhard Haurwitz is also greatly appreciated. Many thanks are due to Mrs. Alice Fields for her assistance with computer programming and to Mrs. Brenda Beattie for typing the manuscript.

The research carried out in this report was supported in part by the U. S. Atomic Energy Commission under Grant No. AT(11-1)-1340.



## TABLE OF CONTENTS

Chapter	Page
ABSTRACT . . . . .	iii
ACKNOWLEDGEMENTS . . . . .	iv
TABLE OF CONTENTS . . . . .	v
LIST OF TABLES . . . . .	vi
LIST OF FIGURES . . . . .	vii
I INTRODUCTION . . . . .	1
II PREVIOUS WORK: A RESPONSE IN THE TROPOSPHERE . . . . .	4
III A REACTION IN THE STRATOSPHERE TO SOLAR VARIABILITY . . . . .	13
A. The Data . . . . .	15
B. The Comparisons . . . . .	16
C. Sector Boundary Events . . . . .	21
IV DOWNWARD PROPAGATION OF STRATOSPHERIC WARMINGS . . . . .	29
V STABILITY OF THE POLAR VORTEX . . . . .	38
VI POSSIBLE MECHANISMS . . . . .	43
A. The Polar Vortex Center . . . . .	43
B. Direct Absorption . . . . .	44
C. Other Approaches . . . . .	48
D. Discussion . . . . .	52
VII CONCLUSION . . . . .	55
REFERENCES . . . . .	56
APPENDICES . . . . .	59



LIST OF TABLES

Table	Page
1. Synopsis of earlier work relating solar flares to tropospheric meteorological phenomena . . . . .	7
2. A comparison of mean values of the 10 millibar 30,640 meter contour mean latitude and standard deviation for specific five day periods preceding and following certain key events . . . . .	42



## LIST OF FIGURES

Figure	Page
<p>1. The inner portion of the figure is a schematic representation of a sector structure of the interplanetary magnetic field that is suggested by observations obtained with the IMP-1 spacecraft in 1963. The plus signs (away from the sun) and minus signs (toward the sun) at the circumference of the figure indicate the direction of the measured interplanetary magnetic field during successive 3-hour intervals. The deviations about the average streaming angle that are actually present are not shown. (After Wilcox and Ness, 1965) . . . . .</p>	10
<p>2. Superposed epoch averages of the daily mean latitude, <math>\phi</math> (top diagram), and the daily standard deviation, <math>\sigma</math> (bottom diagram), of the 30,640 meter contour line at 10 millibars surrounding Key Geomagnetic Dates. Data averaged were taken from 98 cases in 9 cold seasons (November through March) for the years 1960-61 through 1968-69 . . . . .</p>	18
<p>3. Same as Figure 2 except that the data excludes those epochs in which the key date was not preceded by at least nine non-key dates. It also excludes two events for reasons described in the text. The mean values of 38 cases are therefore shown . . . . .</p>	19
<p>4. Same as Figure 3 except that the data are taken from the seasons 1957-58 through 1959-60. Fourteen epochs are used in computing the observed results . . . . .</p>	22
<p>5(a). Superposed epoch averages of the daily area (in arbitrary units) of the cold pool (<math>T \leq -30^{\circ}\text{C}</math>) at 500 millibars surrounding Key Geomagnetic Dates. Such dates (113 in all) were selected from November through March in the seasons 1953-54 through 1962-63 . . . . .</p>	23
<p>5(b). Same as Fig. 5(a) except that Key Dates include only those preceded by at least 9 non-key dates. Forty-five epochs were used in these computations . . . . .</p>	23



LIST OF FIGURES - Continued

Figure	Page
6. The superposed epoch averages of the daily mean latitude ( $\bar{\phi}$ ) and the daily standard deviation ( $\sigma$ ) of the 30,640 meter contour at 10 millibars surrounding Key Sector Dates. Forty-two cases were included from November through March in the seasons 1963-64 through 1968-69 . . . . .	25
7. Area averaged vertical motion ( $\tilde{w}$ ) in $\text{km day}^{-1}$ for indicated periods before, during, and after polar night vortex breakdown of January-February 1958. Hatching denotes area of rising motion. (From Mahlman, 1966) . . .	27
8(a). Superposed epoch averages of mean zonal height at $50^\circ\text{N}$ at the 10, 30, 50, 100 millibar levels surrounding key dates selected according to the Warming I criteria. Each vertical increment represents 20 gpm . . . . .	32
8(b). Superposed epoch averages of mean zonal height at $50^\circ\text{N}$ at the 10, 30, 50, 100 millibar levels surrounding key dates selected according to the Warming II criteria. Each vertical increment represents 20 gpm . . . . .	33
8(c). Superposed epoch averages of mean zonal height at $50^\circ\text{N}$ at the 10, 30, 50, 100 millibar levels surrounding key dates selected according to the Warming III criteria. Each vertical increment represents 20 gpm . . . . .	34
9. Superposed epoch averages of the 30,640 meter contour mean latitude ( $\bar{\phi}$ ) at 10 mb surrounding an increase in mean latitude of 4 degrees or more in 9 days (upper curve). The superposed epoch averages of the area of the cold air ( $T < -30^\circ\text{C}$ ) in arbitrary units surrounding such events are shown in the lower curve . . . . .	36
10. Meridional cross section (over the pole) of the 10 millibar surface surrounding an increase in mean latitude (shrinkage of the polar vortex) of the 30,640 meter contour, if it is associated with large scale warming or subsidence. The solid line represents the 10 millibar heights preceding the shrinkage and the dashed curve represents height values following the shrinkage . . . . .	45
11. Meridional cross section (over the pole) of the 10 millibar surface surrounding an increase in mean latitude (shrinkage of the polar vortex) of the 30,640 meter contour, if it is associated with a steepening of the contour gradient along the vortex edge. The solid line represents the 10 millibar heights preceding the shrinkage, and the dashed curve represents height values following it . . . . .	46



LIST OF FIGURES - Continued

Figure	Page
12. Superposed epoch averages of the 30,640 meter contour mean latitude ( $\bar{\phi}$ ) at 10 mb surrounding an increase in mean latitude of four degrees or more in 9 days (upper curve). The superposed epoch averages of the value (in meters) of the polar vortex central contour at 10 mb are shown on the lower curve . . . . .	47
13. A schematic diagram of two 10 millibar surfaces with latitudinal height gradients of -80 meters per degree latitude . . . . .	50
14. Superposed epoch analyses of average response of hemispheric vorticity area to passing of 54 sector boundaries in the northern hemisphere north of 20°N latitude in which the vorticity exceeded a value of $20 \times 10^{-5} \text{ sec}^{-1}$ are included. The results are shown for pressure levels of 10 mb, 30 mb, 50 mb, and 100 mb. Each graph includes the maximum and minimum values of the vorticity area within the range $\pm 6$ days from sector boundary passage. At the top of each graph is listed the vorticity discriminator in units of $10^{-5} \text{ sec}^{-1}$ , and the minimum, maximum, and range of the vorticity area are in units of $10^5 \text{ km}^2$ . (From Wilcox, et al., 1973) . . . . .	53



## INTRODUCTION

There is little argument that the driving mechanism for the earth's atmospheric motion stems from solar irradiation. Its conversion into potential energy and subsequently into kinetic energy is a subject which is fairly well understood by meteorologists today. The variability of the solar output, especially near the fringes of the solar spectrum, is a subject which is still debated and not fully resolved. The effect of this variability, whatever its magnitude, upon the circulation patterns of the earth's atmosphere as well as on our weather and climate is also open to considerable controversy. Although the effect of the sun's variable output of high energy particles has been generally established in the upper atmosphere (about 100 km and above), the result of the precipitation of the so-called "corpuscular radiation" upon the lower layers is still shrouded in the enormous collection of atmospheric data available today. Researchers for several decades have attempted to extract this information with some degree of success. Statistical correlations of the solar variability with weather and climatic phenomena over a wide range of time and space scales have sometimes been very significant. (For summaries of previous work see Schuurmans, 1969 and Lamb, 1972.) However, the search for a mechanism which can transform the comparatively small energy associated with solar variability into the observed reactions in the troposphere goes on.

The now infamous correlation of the sunspot cycle with the water level of Lake Victoria in Africa (Brooks, 1923) and its subsequent disproof (Lamb, 1972) is but one instance of the statistically small number of data sets which are unrelated but highly correlated according to statistical tests. It is unfortunate that such a plethora of correlations with no physical basis for the observed relation plague this field (Roberts, 1973). The author, however, is a hopeless activist and an optimist. It is believed that a systematic and open minded approach to correlating weather and climatic phenomena with solar/geo-physical variability will be the first step in discerning the mechanism or mechanisms responsible for the observed relations. The aim of such correlations should be to suggest such a mechanism or to disprove or substantiate mechanisms which have already been suggested.

The research presented in this paper has been carried out with these thoughts in mind. It is felt that enough correlations between solar inconstancy and tropospheric weather or climatic observations have already been made. These excite the imagination. They drive the inquisitive into investigating the next logical step along this path, and that is the correlation of solar variability with the atmosphere's kinematics or the flow patterns which produce the observed phenomena. Hopefully this would inspire a systematic inspection of the dynamics of the atmosphere and eventually lead to unravelling the ultimate goal: the mechanism. Our aim is this: to relate the solar variability to the kinematic properties of the stratosphere. Stratospheric levels lie physically between the cause and the effects noted previously. It is entirely possible that the mechanism(s) which bring about the observed correlations would be felt at these levels either through an

intermediary role or as a secondary effect of reactions brought about at other levels. In any case, because of its location, the motion of the stratosphere surrounding events of large solar variability demands to be inspected. This we propose to do.

PREVIOUS WORK: A RESPONSE  
IN THE TROPOSPHERE

One of several parameters may be chosen as an index to solar variability. These may be marked by the following phenomena (Lamb, 1972):

- (a) an index of the occurrence of the flare and its intensity or of flocculi (plages);
- (b) passage of the flare-associated sunspot area across the central solar meridian as seen from the earth and at a solar latitude less than  $15^{\circ}$ ;
- (c) a large disturbance in the ionosphere;
- (d) the greatest associated geomagnetic disturbance (which usually has a "sudden commencement" corresponding to the sharp build-up of the flare); or
- (e) the greatest auroral activity.

Some older research papers, especially those correlating long term effects of solar variability, use records of auroras as an index, but such an approach is highly subjective. Generally the indices used have been (a) and (d) above. Schuurmans (1969) argues that the flare approach, (a), is preferable because some fluctuations in the geomagnetic indices, (d), can be attributed to geophysical phenomena, and consequently a statistical relationship between geomagnetic disturbances and some weather element does not imply that that element is

influenced by extraterrestrial forces. Knecht (1972) states that except for some minor fluctuations in the motions of the upper atmosphere the sun is responsible for all significant geomagnetic disturbances recognized at present. Lamb and Schuurmans (op. cit.) both agree, however, that the geomagnetic index has the advantage of reflecting the actual existence of a solar influence upon the earth's atmosphere. Sudden fluctuations in the geomagnetic field strength usually result from abrupt changes in the direction or intensity of the interplanetary magnetic field, or they result from abrupt changes in the density or velocity of the solar wind. Such changes are usually associated with flare activity (Knecht, 1972), and regardless of the preferred approach, one is quantifying the same solar inconstancy in the mean. We will use the so-called geomagnetic index as an indication of this variability in the sun's output. The method of formulating this index will be described later.

Before proceeding with a discussion of our work, we will present a brief summary of some recent research papers on this subject. Schuurmans (1969) gives one summary of investigations which correlated solar flare activity with various tropospheric events. This summary is presented in Table 1. Notice the positive correlation, along with some time lag, between the flares and pressure level height rises, surface pressure increases, temperature increases, and precipitation augmentation. Only Hartman (1963) considers a global effect; however, his data cover but one event. The results of some other recent work relating this variability to meteorological phenomena in the lower atmosphere will be presented.

Macdonald and Roberts (1960) and Roberts and Olson (1973a,b) have noted that 300 millibar troughs which enter the Gulf of Alaska 1 - 3 days after a geomagnetic storm tend to intensify to a greater degree than those troughs which enter that same area at other times. In addition, they note that such key troughs, if tracked further, tend to be more intense than the others as they move across eastern North America several days later.

Shapiro (1956, 1959, 1972) has shown that the persistence of sea level pressures over several mid-latitude regions was greater following a geomagnetic storm than at other times. Stolov and Shapiro (1969) and Shapiro and Stolov (1970), however, show that there is no correlation between solar variability and surface pressures in the polar regions. These authors used solar flares as their index of solar activity.

Jagannathan and Bhalme (1973) relate characteristics of the Southwest Monsoon over India to the solar sunspot cycle. They show that the years of maximum rainfall may be associated with sunspot maximum or minimum, depending upon location. The duration and intensity of rainy spells as well as breaks in the monsoon appear to have a periodicity associated with the solar cycle.

In studying the effects of solar flare activity on the northern hemisphere, Schuurmans (1969) noted a mean increase in the height of constant pressure surfaces, with the maximum increase at 300 millibars, in the troposphere over mid-latitudes. At higher latitudes, poleward of 70°N, he discovers that the mean height of these pressure surfaces drops. Equatorward of 45°N a slight increase in height of these

TABLE 1

Synopsis of earlier work relating solar flares to tropospheric phenomena (from Schuurmans, 1969).

author	No. of flares	period	atmospheric parameter	geographical region	results
DUELL and DUELL (1948)	51	1936-41	500 mbar heights	European-Atlantic region between	mean height rise of the 500 mbar level (max. + 1 gpdm over the North Sea and adjacent areas) from the day before the flare to the day of the outburst.
DUELL and DUELL (1948)	51	1936-41	sea level pressure	3 stations in Central Europe	maximum of interdiurnal pressure change between 2-4 days after a flare; maximum of pressure itself 4-6 days after a flare.
VALNICEK (1952)	69	1936(33) 1947(36)	pressure and temperature at ground level	Eastern Atlantic and Europe	SE-ward displacement of the polar front, 2-5 days after a flare, displacement being accompanied by a change in circulation regime from zonal to meridional.
VALNICEK (1953)	53	1949-50	500 mbar heights	Eastern Atlantic and Europe	mean height rise of the 500 mbar level (max. + 5 gpdm over North Sea-southern Scandinavia) between the fifth day before the flare to the day of the flare outburst.

TABLE 1 (Continued)

author	No. of flares	period	atmospheric parameter	geographical region	results
NORDØ (1953)	115	July 1935 -- June 1952	sea level pressure	Oslo (Norway)	significantly positive 24-hour pressure tendencies during the first day after strong isolated flares, occurring in winter at night time. (in NORDØ'S opinion the evidence is not convincing).
PALMER (1953)	?	March through May 1951	temperatures in the lower stratosphere	equatorial regions (Marshall Islands)	temperature rise of about 7°C per day at a level close to the tropopause, with a delay of less than 36 hours after a flare. ∞
ATTMANNSPACHER (1955)	30	Jan. 1951 -- June 1952	temperature at 96, 41 and 15 mbar	Berlin	temperature rise during the first 24 hours after a flare of the order of 1°C, increasing with increasing height of the pressure level.
HARTMANN (1963)	1	June 1, 1960	temperature of the 500 mbar level	whole northern hemisphere	temperature rise (area-mean of the hemisphere) of 4°C from June 1 to June 2.
KUBISHKIN (1966)	41	1956-61	ground level pressure	94 northern hemisphere stations (43 in USSR) and 9 stations in Angola (Africa)	pressure reaches an extreme on the third to fourth day after a flare, the sign of the extreme depending on the location of the station.

TABLE 1 (Continued)

author	No. of flares	period	atmospheric parameter	geographical region	results
TAKAHASHI (1966)	54	1957-63	amount and frequency of occurrence of precipitation	5 Japanese stations	increase of precipitation on the day of the flare outburst.
STOLOV and SPAR (1968)	41*	1956-61	ground level pressure	31 stations in North America	no statistical significant pressure departures following the flares.

\*KUBISHKIN'S list of flares.

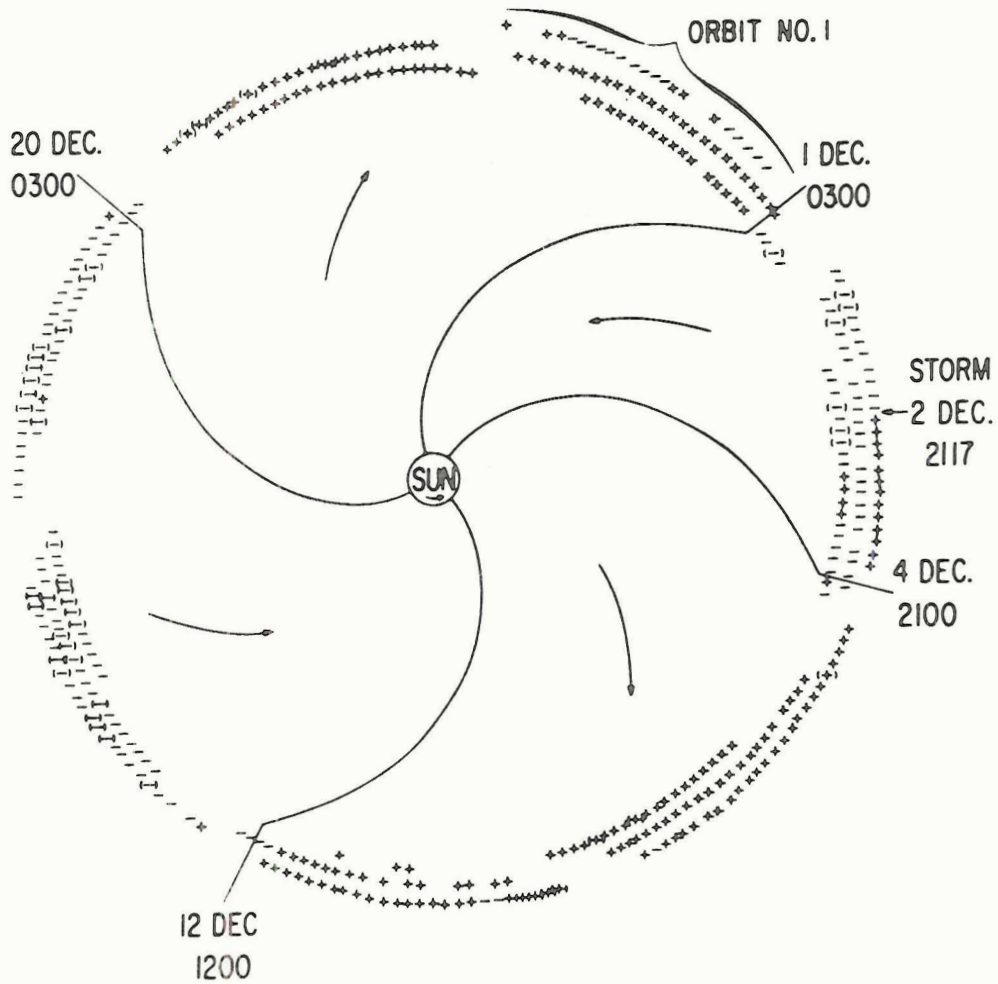


Figure 1. The inner portion of the figure is a schematic representation of a sector structure of the interplanetary magnetic field that is suggested by observations obtained with the IMP-1 spacecraft in 1963. The plus signs (away from the sun) and minus signs (toward the sun) at the circumference of the figure indicate the direction of the measured interplanetary magnetic field during successive 3-hour intervals. The deviations about the average streaming angle that are actually present are not shown. (After Wilcox and Ness, 1965).

pressure surfaces is noted. All these phenomena are observed to occur from one to three days following the appearance of a solar flare.

In yet another form of variability in the solar output, Wilcox and Ness (1965) describe a solar magnetic structure depicted in Figure 1. This structure consists of usually four sectors in the ecliptic plane in which the interplanetary field is generally directed either toward or away from the sun. The boundaries of these sectors sweep past the earth as the sun and the interplanetary magnetic field rotate. Wilcox et al. (1973) describe the variations observed in the solar output as these boundaries overtake the Earth in its orbit. They note a decrease in solar flux preceding boundary passage with generally higher flux after it. They also discover that the average vorticity in the troposphere north of 20°N latitude reaches a minimum approximately one day after the passage of a sector boundary and that this mean vorticity increases during the next two or three days.

In this summary, we have mainly considered the long term climatic effects of the solar variability. Lamb (1972) gives a comprehensive summary of research which tackles this problem. In addition, Wollin et al. (1973) show correlations between total magnetic intensity and short period climatic changes on a geographical basis. Tentatively, they conclude that trends in intensity of the magnetic field tend to correlate negatively with ten year means of air temperature. Moreover, they realize that both processes may proceed from parallel reactions to solar variability. Sinno and Higashimura (1969) and Shapley and Beynon (1965), among others, correlate stratospheric warmings and  $f_{\min}$ , the minimum reflected frequency of the ionosphere, but this phenomena will not be discussed further here.

In summary, the literature abounds with correlations between solar variability and several tropospheric parameters. Some of these correlations have been high while others have not. In addition, the possibility of spurious correlations in some results must be considered. Several researchers discuss or speculate about a mechanism which can carry out the observed reactions, but there appears to be little agreement on the relative importance or feasibility of the mechanisms. These will be presented in a later section.

## A REACTION IN THE STRATOSPHERE TO SOLAR VARIABILITY

Only a few researchers have even briefly mentioned a possible reaction of stratospheric flow to solar variability. Manson (1969) studies the 1963 final spring warming in the antarctic and concludes that there is insufficient atmospheric data to confirm the hypothesis that stratospheric warmings are triggered by solar particle influx. He mentions that a more detailed knowledge of the photochemistry of ozone at heights up to 110 km is needed. Willett (1968) compares stratospheric warmings and total ozone variability in both the arctic and antarctic stratosphere and concludes that solar corpuscular radiation along with the initial state of flow may account for the observed differences in the two regimes. Labitzke (1964) detects a warming in the stratosphere at 10 millibars following a geomagnetic storm, but notes that such warmings are not perceived at lower levels. Wilcox et al. (1973) discover that in the lower stratosphere their "vorticity area index," which is related to the area and intensity of cyclones and troughs, shows a minimum near the time of a passing of a sector boundary with numerically increasing values two or three days later. This effect is most prominent at mid-latitudes but is not detectible at mid-levels in the stratosphere. Schuurmans (1969) observed that no changes in the height of pressure surfaces in the lower stratosphere occurred following flare activity. London et al. (1959) show that over a five year period over the United States, any correlation between

geomagnetic variations and 100 millibar height gradients is either negligibly small or nonexistent. Ward (1960) concludes that any correlation between solar variability and 100 millibar temperatures is at best barely detectible. Such results are either inconclusive or discouraging to one who attempts to promote a reaction in the stratosphere to the sun's inconstancy. None of these papers deals with the reaction of the polar night vortex over a large number of events, however; and we will deal with this problem.

With this in mind, we will embark on a statistical exploration of stratospheric flow which is associated with the size and shape of the polar vortex. In particular we will define such parameters for the flow at 10 millibars and attempt to deduce whether warmings detected at this level can be observed at other levels. We will confine ourselves to the northern hemisphere mid-latitudes and polar latitudes during the months of November through March (in this paper called the "cold season"). A set of data dealing with the 500 millibar level over the northern hemisphere during these time periods will also be studied.

The superposed epoch method was used to investigate relationships between the variations of solar output and flow in the atmosphere. This method compares two sets of data: key events are selected from one set, and the values of the other set which surround all such events are noted and averaged. In this paper, twenty-nine days surrounding each key event are used in a single epoch. These range from the fourteenth day preceding an event to the fourteenth day following it. These dates are noted as  $D_{-14}$ ,  $D_{-13}$ , ...,  $D_{-1}$ ,  $D_0$ ,  $D_1$ , ...,  $D_{14}$ . The key event occurs on  $D_0$ . In this section we employed

a set of indices of geomagnetic activity to be used in determining the key events. We developed two separate sets of data of "reacting" events, one dealing with the polar troposphere and the other with the polar stratosphere. These three sets of data will be described first, and their comparisons and results using the superposed epoch method will follow.

#### 1. The Data.

To develop an objective method for determining a sudden increase in geomagnetic activity, we used the daily planetary geomagnetic activity index,  $A_p$ , as published by the National Geophysical and Solar-Terrestrial Data Center. This is a daily global index of geomagnetic activity which varies directly with the severity of the storm. Key dates of this activity, called "Geomagnetic Key Dates" were selected according to two criteria: The daily  $A_p$  value must be greater than or equal to 15, and the increase from the previous daily value must be at least as large as the monthly average value of  $A_p$ . These are the same two criteria used in the paper by Roberts and Olson (1973). The key dates cover seventeen years from 1953 through 1969 and therefore are available for all winters for which we have tropospheric and stratospheric data available.

Our set of data for the stratosphere parameterizes the size and convolution of the polar vortex at 10 millibars. It is identical to that used in the previous study by Reiter and Macdonald (1973). The 30,640 meter contour at this pressure level generally lies near the edge of the polar vortex during the months from November through March. The latitude value of this contour at  $30^\circ$ -longitude intervals is noted

for each day, giving twelve such values. The mean of these latitudes gives a rough idea of the areal extent, although not of the intensity, of the vortex. The standard deviation of these values gives an indication of the convolution or meridionality of the vortex flow. For each day in twelve cold seasons (November through March), 1957-58 through 1968-69, we obtained a mean latitude value as well as a standard deviation value for this contour line.

The tropospheric data deal with the daily size of the 500 millibar cold pool. Generally the  $-30^{\circ}\text{C}$  isotherm lies near the polar front at this level, and the area enclosed by this isotherm should give an indication of the areal extent of the cold pool. We planimetered the area enclosed by this isotherm from maps published by the U. S. Weather Bureau for each day in ten cold season 1953-54 through 1962-63. Values for two of the seasons, 1961-62 and 1962-63, were taken from operational charts while the others were taken from the Daily Series Synoptic Weather Maps published by the U. S. Weather Bureau. Portions of this area which occasionally broke away from the main cold pool were disregarded unless they "rejoined" the pool at a later time. This data set consists of the daily area of the 500 millibar cold pool in arbitrary units.

## 2. The Comparisons.

First let us compare the Geomagnetic Key Dates with the mean latitude and standard deviation of the polar vortex, our stratospheric data. Ninety-eight key dates based on the criteria already given in (1.) were selected from nine cold seasons, 1960-61 through 1968-69. The mean values of these two sets of stratospheric data for the 98

epochs surrounding the key events are shown in Figure 2. Note the significant increase in mean latitude of the 30,640 meter contour, indicating a shrinkage of the polar vortex, from the third to the eighth day following the geomagnetic event. The Wilcoxon Rank-Sum Test shows that the  $D_1$  through  $D_{14}$  mean latitudes are statistically separate from the  $D_{-14}$  through  $D_{-1}$  means at the 99 per cent significance level. Most perplexing is the slight increase in mean latitude along with a corresponding sharp increase in standard deviation preceding the key date. To investigate this situation, we reduced our key dates to only those which were preceded by at least nine non-key dates. This eliminates the "pre event" compounding effects of sequences of key events. Forty key dates met this new criterion. It was noticed, however, that a sudden break-up of the polar vortex circulation occurred during two of these epochs: the mean latitude of the 30,649 meter contour fluctuated by as much as  $20^\circ$  latitude in one day for these two cases. After eliminating these sequences, we are left with the mean values of 38 epochs, and these are shown in Figure 3. Note the rapid increase in mean latitude from  $D_3$  through  $D_7$ . Also, the standard deviation of the vortex jumps most markedly from  $D_5$  through  $D_8$ . These figures indicate that a four to five day shrinkage of the polar vortex at the 10 millibar level follows a Key Geomagnetic Date by about three days, with a slight increase in the ellipticity of, or meridional transport by, the polar vortex later in the period of the shrinkage.

Returning to the 98 original epochs and taking them individually, we tried to determine the statistical significance of the  $D_7$  through  $D_{11}$  mean latitudes compared with some pre-key event values.

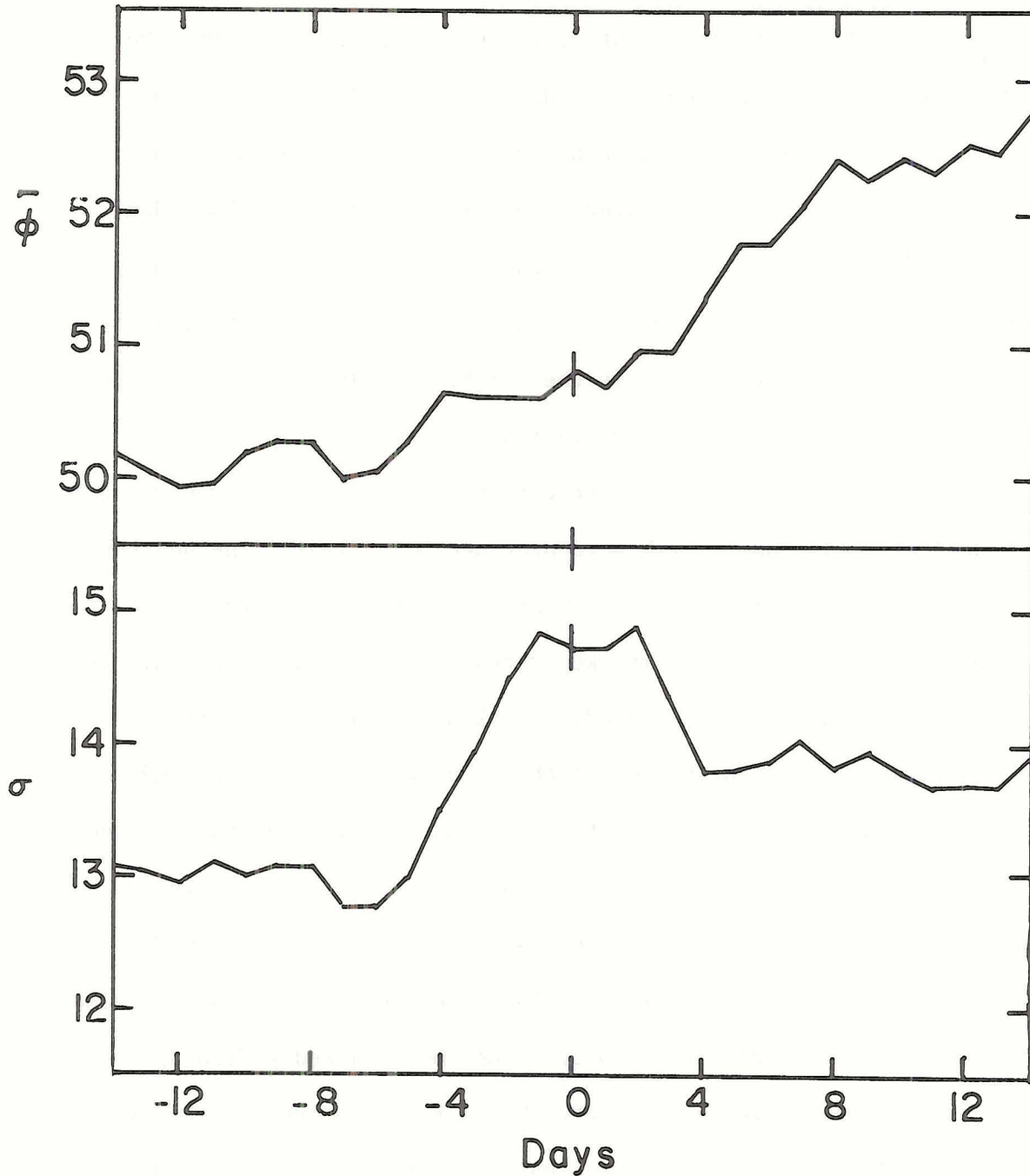


Figure 2. Superposed epoch averages of the daily mean latitude,  $\phi$  (top diagram), and the daily standard deviation,  $\sigma$  (bottom diagram), of the 30,640 meter contour line at 10 millibars surrounding Key Geomagnetic Dates. Data averaged were taken from 98 cases in 9 cold seasons (November through March) for the years 1960-61 through 1968-69.

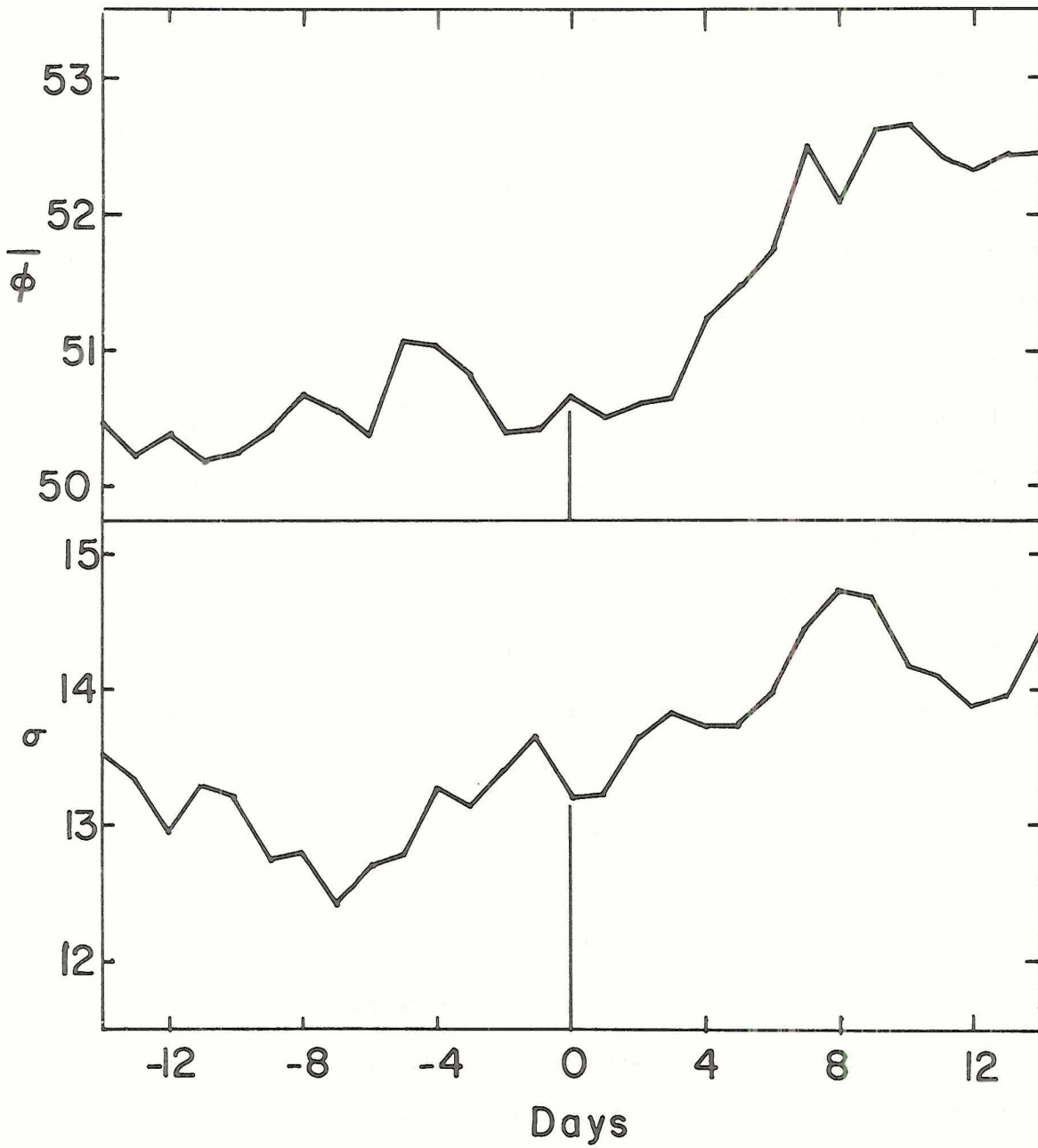


Figure 3. Same as Figure 2 except that the data excludes those epochs in which the key date was not preceded by at least nine non-key dates. It also excludes two events for reasons described in the text. The mean values of 38 cases are therefore shown.

Specifically, we used the  $D_{-10}$  through  $D_{-1}$  mean latitudes for the pre-event calculations, giving a total of fifteen values to be compared for each epoch. A simple rank sum test was used to compare these two sets of data and to determine the statistical significance of their separation. In 52 of the 98 epochs the mean latitude of the  $D_7$  through  $D_{11}$  data is greater than the pre-event values at the 95 per cent significance level. In other words, in more than half of the key epochs this  $D_7$  through  $D_{11}$  increase in mean latitude following the key event is significant.

Three seasons with stratospheric and geomagnetic data (1957-58 through 1959-60) remain, and we used this data to determine whether the same trend will develop from new, independent data. Thirty-one key Geomagnetic Dates were chosen from this sample. Again we selected only those key dates which were preceded by at least nine non-key dates. Fourteen cases remained, and the results of the superposed epoch analysis for these events are shown in Figure 4. Note a similar trend toward an increase in mean latitude following the geomagnetic event (in this case from six to eight days following the key date). The large increase in standard deviation preceding the key date is due mostly to a single event, while the increase preceding  $D_8$  is more general. Of course the data sample size is small, but we merely wish to confirm the results obtained from the previously studied nine-year sample.

Also we tried to determine a mean 500 millibar cold pool response surrounding similar geomagnetic events. Since the tropospheric data and the stratospheric data cover different seasons, the key dates are not exactly the same, however the criteria used in selecting them

remain identical. The ten cold seasons which were used ran from 1953-54 through 1962-63, and 113 days were selected as Key Geomagnetic Dates from this period. The mean values of the area within the  $-30^{\circ}\text{C}$  isotherm surrounding the key dates are shown in Figure 5(a). No statistically significant variation can be determined from this data. Selecting only those key dates which were preceded by at least nine non-key dates, we noted the mean area variations which are given in Figure 5(b). Again, no significant variation is apparent. We are, therefore, unable to detect any significant variation in the size of the 500 millibar cold pool following a period of increased solar activity.

### 3. Sector Boundary Events.

Occasionally, and often at the time of a geomagnetic storm, the orientation of the interplanetary magnetic field switches (Wilcox and Ness, 1965). Wilcox et al. (1973) observed a vorticity minimum in the troposphere and lower stratosphere north of  $20^{\circ}\text{N}$  latitude about one day after the passage of a sector boundary of the interplanetary magnetic field. No overlap of our tropospheric data and the years for which we have sector data available occurred, but we thought it might prove interesting to determine whether such an event had an effect on the circulation of the stratospheric polar vortex at 10 millibars. Forty-two dates of sector boundary passage, irrespective of the direction of the switch in orientation of the interplanetary field, were selected from the cold seasons from 1963-64 through 1968-69. These were called Sector Key Dates, and the superposed epoch method was used to determine a mean stratospheric reaction surrounding these

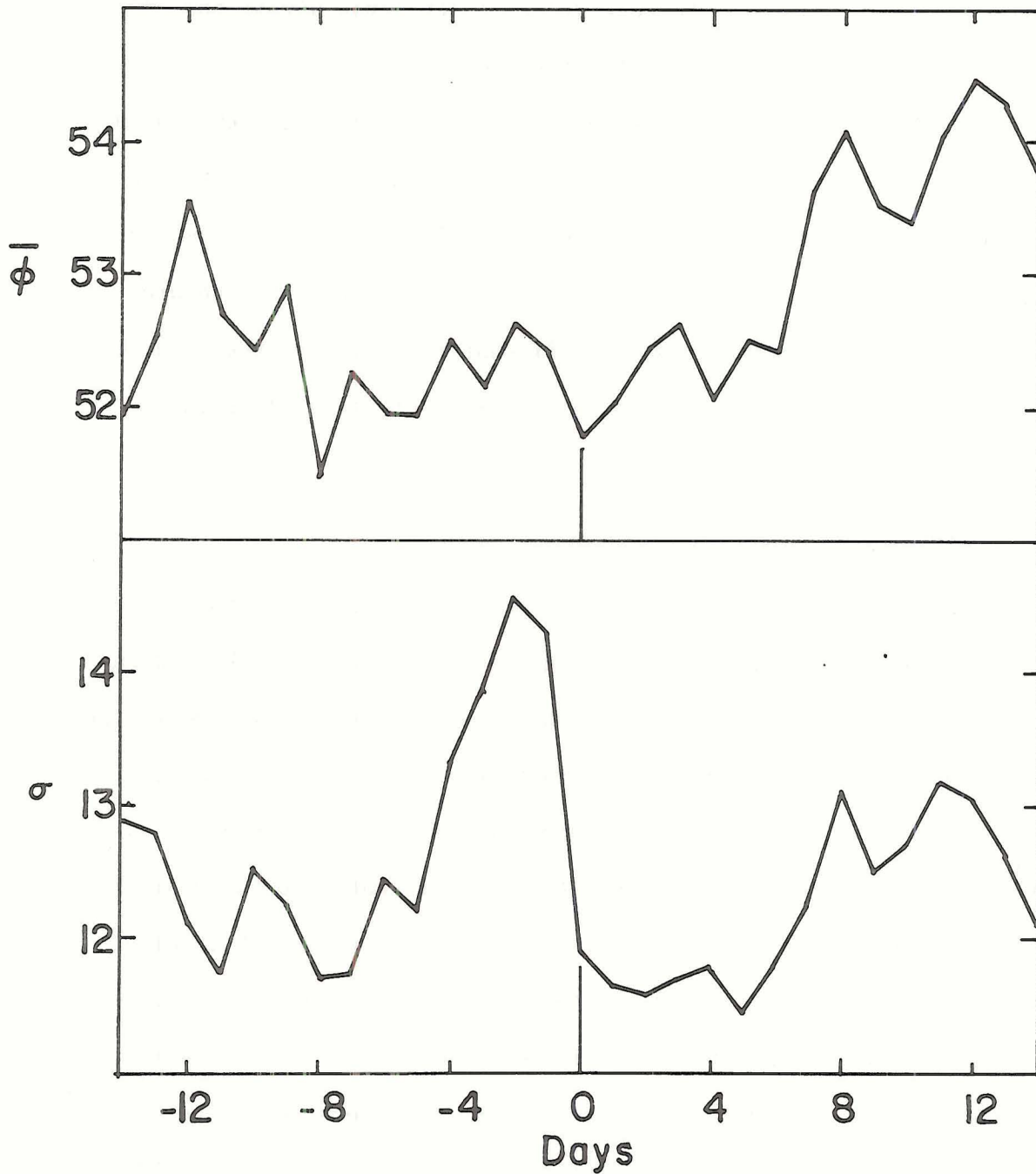


Figure 4. Same as Figure 3 except that the data are taken from the seasons 1957-58 through 1959-60. Fourteen epochs are used in computing the observed results.

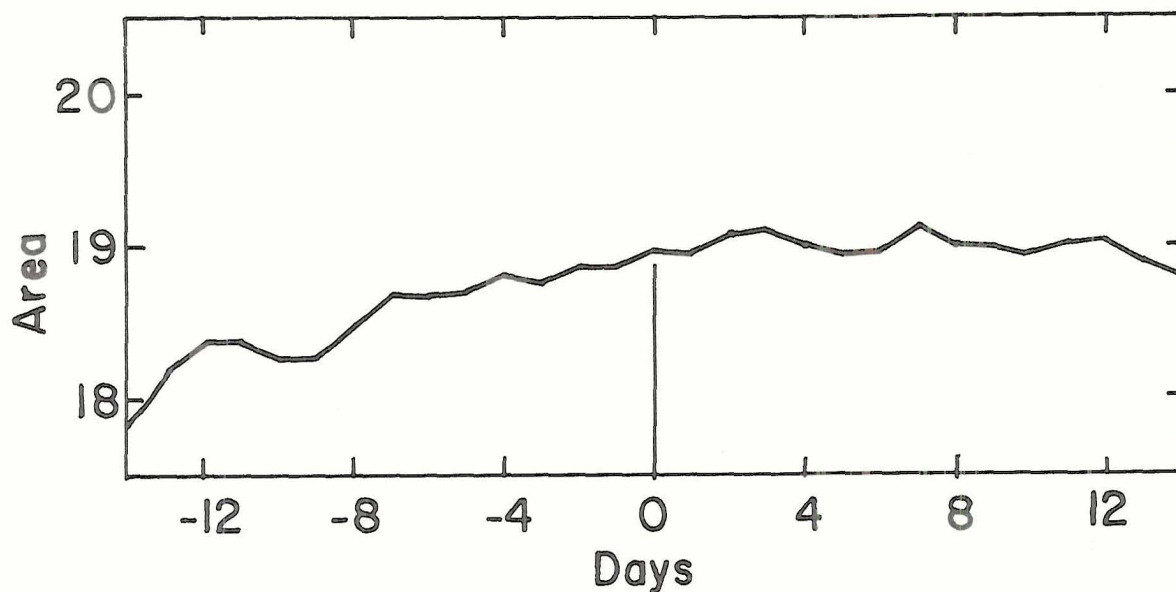


Figure 5(a). Superposed epoch averages of the daily area (in arbitrary units) of the cold pool ( $T < 30^{\circ}\text{C}$ ) at 500 millibars surrounding Key Geomagnetic Dates. Such dates (113 in all) were selected from November through March in the seasons 1953-54 through 1962-63.

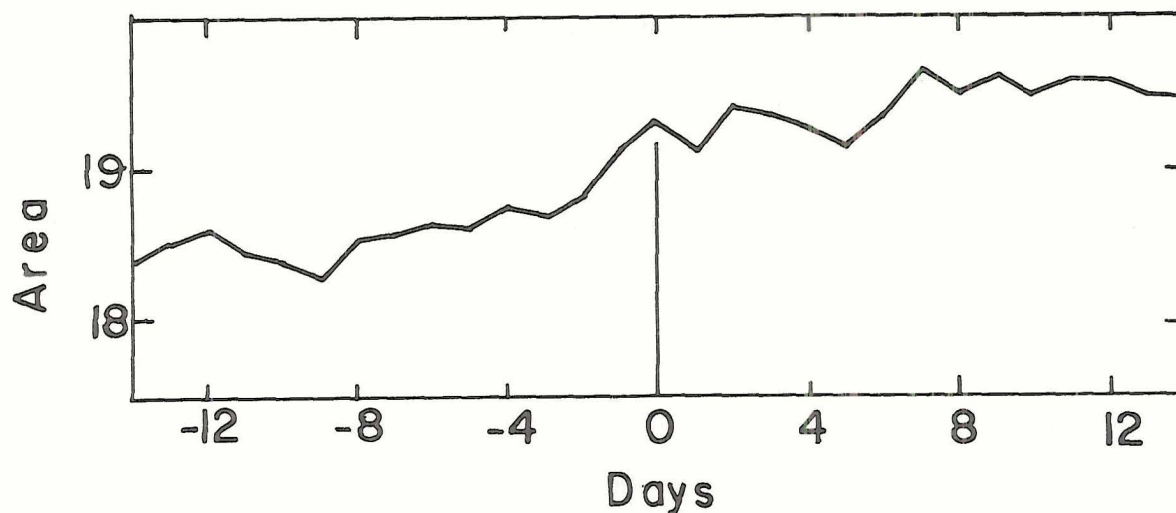


Figure 5(b). Same as Fig. 5(a) except that Key Dates include only those preceded by at least 9 non-key dates. Forty-five epochs were used in these computations.

dates. The mean of the 30,640 meter contour mean latitude and the mean of its standard deviation surrounding these events are shown in Figure 6. Note the slight decrease in mean latitude (expansion of the polar vortex) following the key date, with relatively lower values of mean latitude from  $D_3$  through  $D_7$ .

Using a simple rank sum test, we compared the values for these five days with those of the  $D_{-10}$  through  $D_{-1}$  segment separately for each of the forty-two epochs. In fourteen of the cases, the  $D_3$  through  $D_7$  sample was lower than the pre-key date sample at the 95 per cent significance level. In sixteen of the cases, however, this  $D_3$  through  $D_7$  sample was actually greater than the pre key date sample above the 95 per cent significance level. Thus we could establish no statistically significant trend.

From the results presented in this section, one can conclude that the polar vortex edge at 10 millibars appears to warm, or at least to steepen its contour gradient, after a period of rapid increase in solar activity detected on earth. The selection of key dates which were preceded by at least nine non-key dates and the elimination of cases which were associated with a major readjustment in vortex flow were used in discerning this reaction. These are the basic factors which we used to eliminate certain key dates from our sample. One might also infer from Figure 3 that as this warming occurs, there is an increase in the meridional component of the geostrophic flow near the vortex edge. Mahlman (1966) shows that during a sudden warming in the stratosphere (more severe than our events) the vertical motion pattern in the lower stratosphere intensifies but does not change direction. (See Figure 7.) In order to obtain a warming over the

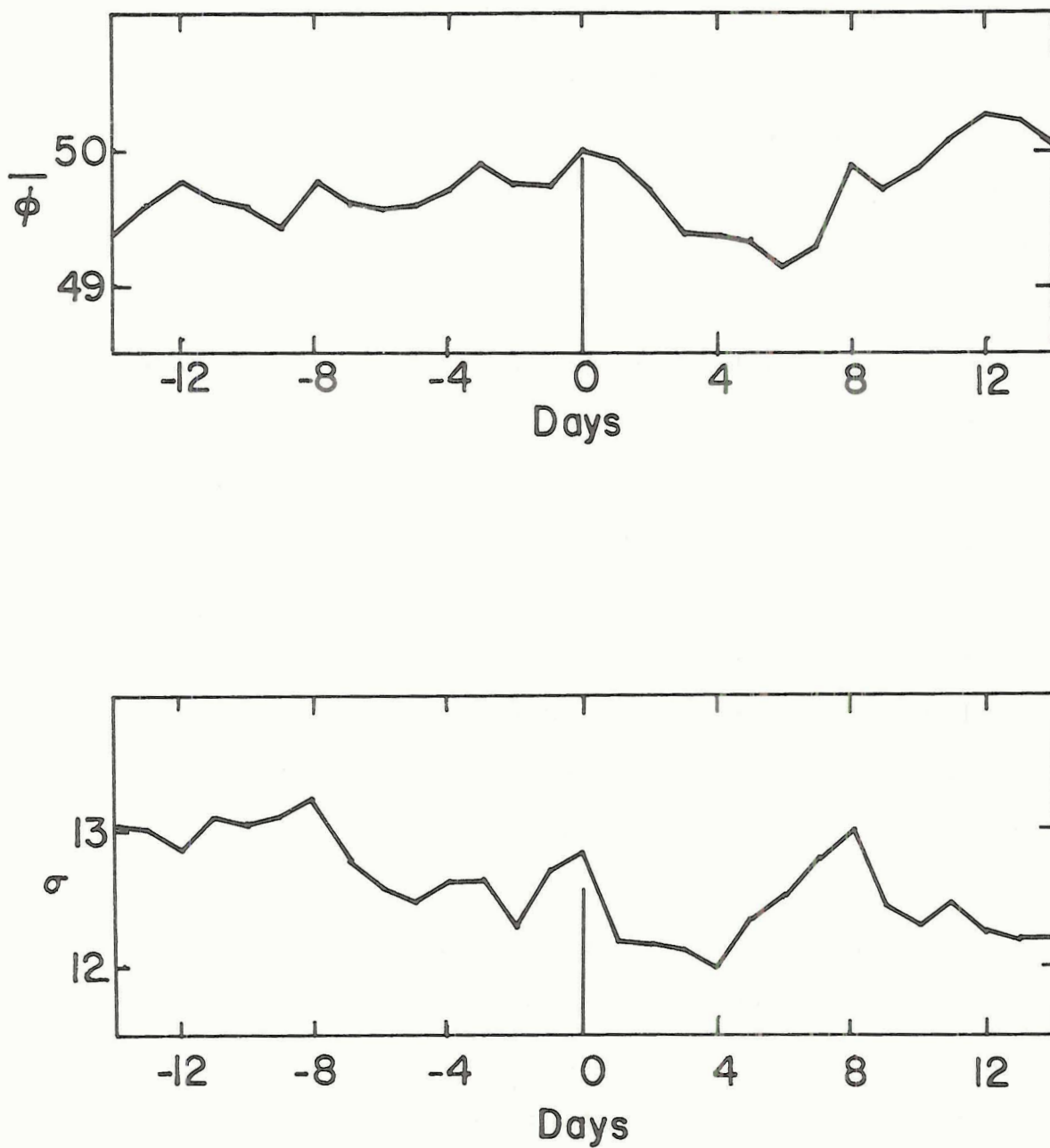


Figure 6. The superposed epoch averages of the daily mean latitude ( $\bar{\phi}$ ) and the daily standard deviation ( $\sigma$ ) of the 30,640 meter contour at 10 millibars surrounding Key Sector Dates. Forty-two cases were included from November through March in the seasons 1963-64 through 1968-69.

pole, therefore, the heating must be supplied by horizontal advection, although there could be localized subsidence in this region. Our detected increase in the meridional component of stratospheric flow may be associated with this horizontal advection. One might infer from Figure 7, however, that an increase in the intensity of the subsiding air over mid-latitudes could produce an increase in temperature near the vortex edge. Horizontal advection of warmer air as well as intensified subsidence probably both play a role in our detected warmings.

The fact that no response is found in the area of the 500 millibar cold pool represents a challenge which will be undertaken in the next section. Certainly the increase in height noted by Schuurmans (1969) of all tropospheric pressure levels in mid-latitudes along with the decrease in height of these same pressure surfaces at high latitudes would suggest a detectable reaction in the 500 millibar cold pool size. Schuurmans (*op. cit.*) uses solar flare occurrence as his index of activity, and he attempts to show calculations which suggest a mechanism taking place at the tropopause level, bypassing any heating of higher levels which would contribute significantly to tropospheric effects. He suggests that height rises in mid-latitudes near the tropopause are propagated to the surface in a matter of three days. Schuurmans' mechanism will be discussed later, but it is frustrating indeed that we can observe no such companion trend in our results.

The lack of a statistically significant variation in stratospheric flow surrounding the passage of a sector boundary is also somewhat confusing. According to Wilcox et al. (1973) there was no difference

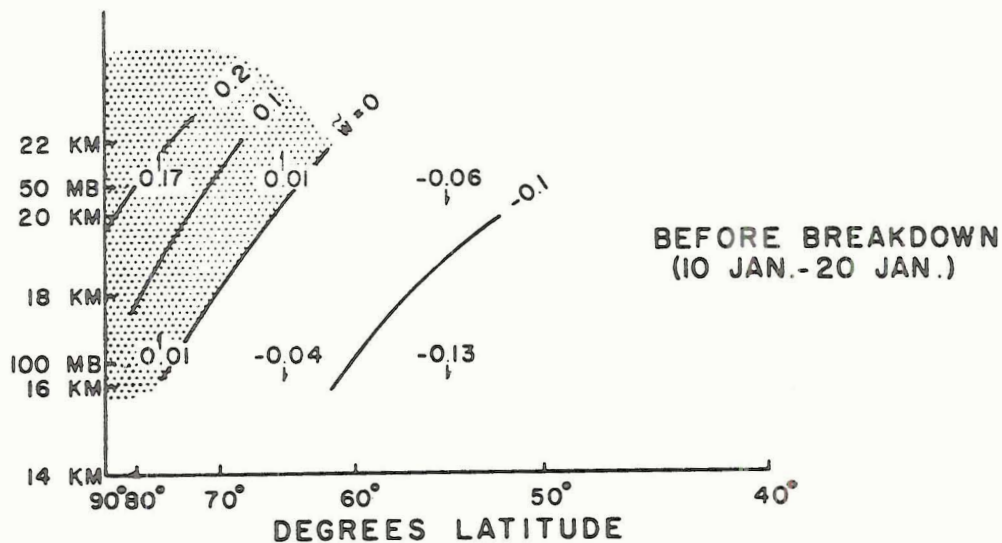
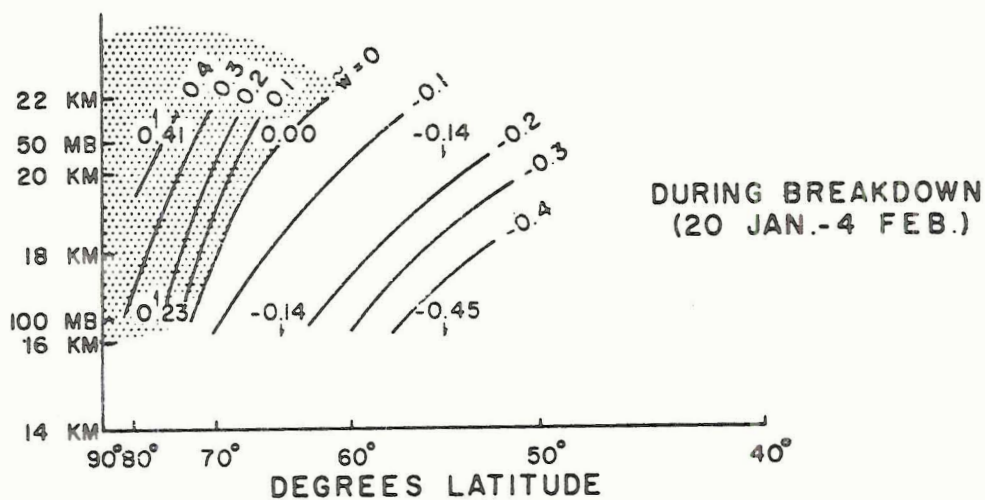
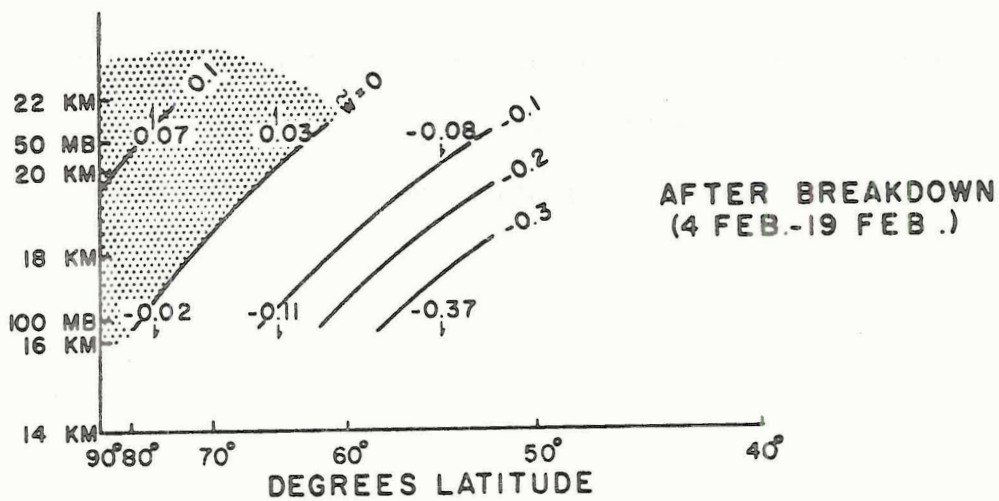


Figure 7. Area averaged vertical motion ( $\tilde{w}$ ) in  $\text{km day}^{-1}$  for indicated periods before, during, and after polar night vortex breakdown of January-February 1958. Hatching denotes area of rising motion. (From Mahlman, 1966).

in their results when they separated their data into two categories according to the direction of the switch in orientation of the interplanetary magnetic field. This problem should not affect our results either.

## DOWNWARD PROPAGATION OF STRATOSPHERIC WARMINGS

It is somewhat perplexing that there is no apparent global response in the troposphere to solar variability according to our results. Other authors (Schuurmans, 1969; Wilcox et al., 1973) have, however, found one. Labitzke (1964) has detected some warmings at 10 millibars which did not penetrate even as low as 30 millibars. Reiter and Macdonald (1973) indicate that the troposphere reacts to sudden, strong warmings in the stratosphere and that these tropospheric warmings tend to occur about two days later. Reiter (1963) shows that a strong pressure surface rise at 15 millibars may propagate downward and be noticed at the 100 millibar level several days later.

In this section, we will take warmings which were perceived at 10 millibars near the polar vortex edge and attempt to discern whether such warmings are propagated downward both into the lower stratosphere and into the troposphere. Our path will be to select key dates of warming at the 10 millibar level and plot the mean heights of the remaining stratospheric pressure surfaces both preceding and following the key event. Three separate sets of warming criteria will be employed in order to study the effects separately of weak, moderate, and strong warmings. Height data was available for the 10, 30, 50, and 100 millibar pressure levels on the standard NMC Octagonal Grid for each month (November through March) of five cold seasons, 1964-65 through 1968-69. Using heights of these surfaces interpolated for a

10° latitude by 10° longitude grid, we calculated zonal mean heights and zonal standard deviations of height values for each day of the five cold seasons.

Several different criteria for a warming event were used, but all dealt with a series of three three-day mean height values during every possible overlapping nine-day sequence throughout the cold season.

Let  $\Delta H_1$  and  $\Delta H_2$  be defined as follows:

$$\Delta H_1 = [(h_4 + h_5 + h_6)/3 - (h_1 + h_2 + h_3)/3]$$

$$\Delta H_2 = [(h_9 + h_8 + h_7)/3 - (h_4 + h_5 + h_6)/3]$$

where  $h_i$  represents the zonally averaged height of the 10 millibar surface at a selected latitude on the  $i$ th day of the nine-day sequence. The classes of the warmings and the criteria used to select them are as follows:

Warming I:  $10 \text{ gpm} \leq \Delta H_1 < 50 \text{ gpm}$  and  $10 \text{ gpm} \leq \Delta H_2 < 50 \text{ gpm}$

Warming II:  $50 \text{ gpm} \leq \Delta H_i < 90 \text{ gpm}$  and  $10 \text{ gpm} \leq \Delta H_j < 90 \text{ gpm}$

where  $i, j = 1 \text{ or } 2$

Warming III:  $90 \text{ gpm} \leq \Delta H_i$  and  $10 \text{ gpm} \leq \Delta H_j$

where  $i, j = 1 \text{ or } 2$

Clearly, the Warming III events are the most intense and the Warming I events are the weakest. The key date of each warming sequence, when the criteria are met, is arbitrarily chosen as the middle day (the fifth day) of the nine-day sequence.

Applying these criteria to zonal height averages at  $50^{\circ}\text{N}$  and  $60^{\circ}\text{N}$  and selecting the key dates, we will calculate the mean variation in zonal height averages at all four of the previously noted levels.

Figure 8 shows the height variations of the four pressure levels at  $50^{\circ}\text{N}$  for warmings detected at 10 millibars during the seasons 1964-65 through 1968-69. Figure 8(a) indicates the mean values of 24 cases which met Warming I criteria. Figure 8(b) depicts the mean fluctuations of the 77 cases which met Warming II criteria, and Figure 8(c) shows the height changes for the 42 Warming III events. Results of warmings at  $60^{\circ}\text{N}$  were similar to those of the  $50^{\circ}\text{N}$  group and are not presented here. It should be noted that the key warming dates for both these latitudes tended to coincide and that warmings determined strictly at one latitude tended to show downward propagation at other latitudes. An increase in the latitudinal standard deviation of height values tends to occur prior to the warming event at both  $50^{\circ}\text{N}$  and at  $60^{\circ}\text{N}$ . This again implies that horizontal meridional transport of heat may be at least partially responsible for warmings in the middle stratosphere. In Figure 8 notice that the increase in height of these surfaces propagates downward from the 10 millibar level. Such warmings are, however, barely detectible at the 100 millibar surface for the weakest (Warming I) cases. These figures suggest that warmings which were evident near the polar vortex edge probably will be felt at lower levels in the stratosphere with a delay of several days.

To approach the problem of relating these 10 millibar warmings to the troposphere, we used the 30,640 meter contour mean latitude data for selecting key events. The 500 millibar cold pool area data,

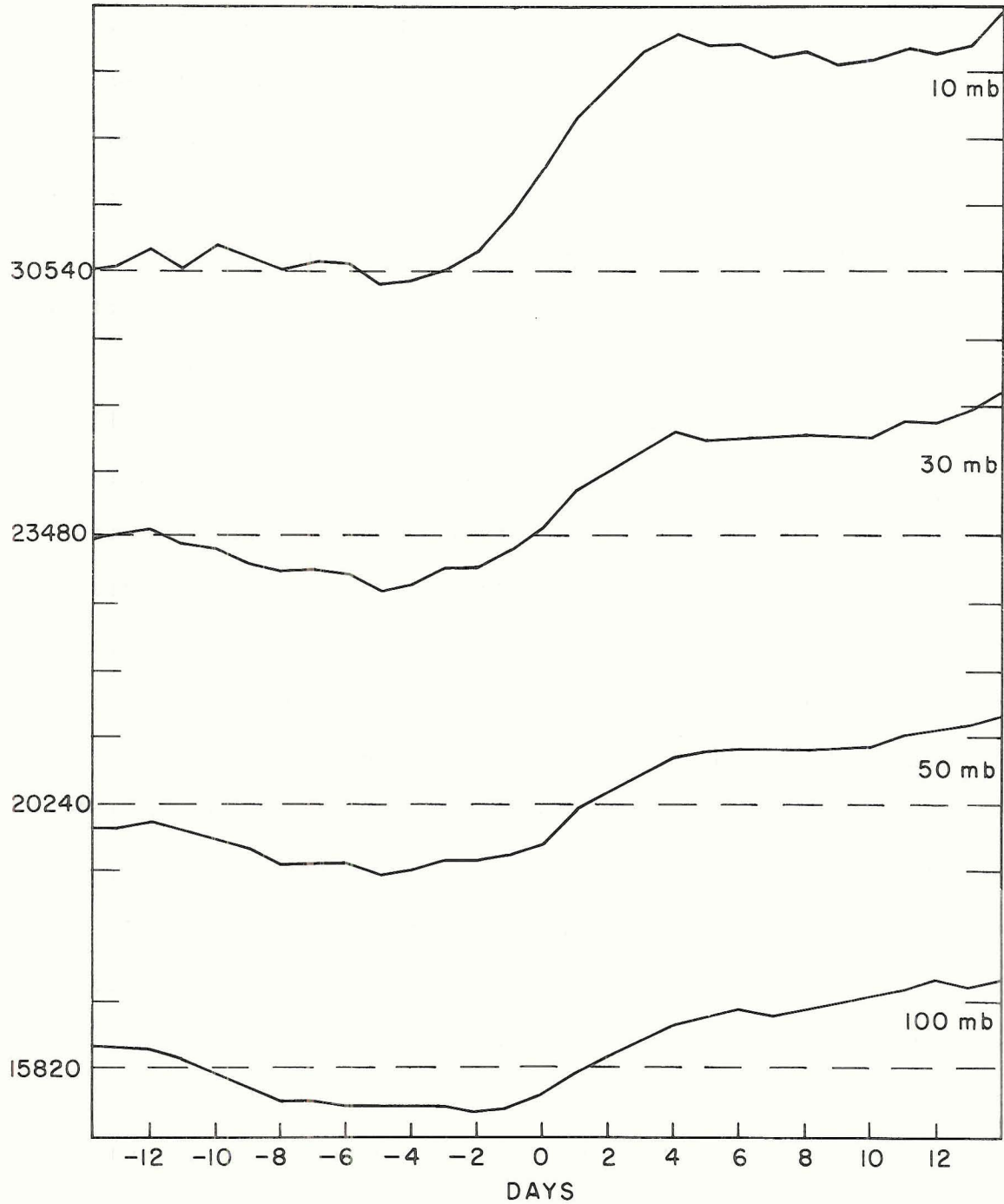


Figure 8(a). Superposed epoch averages of mean zonal height at  $50^{\circ}\text{N}$  at the 10, 30, 50, 100 millibar levels surrounding key dates selected according to the Warming I criteria. Each vertical increment represents 20 gpm.

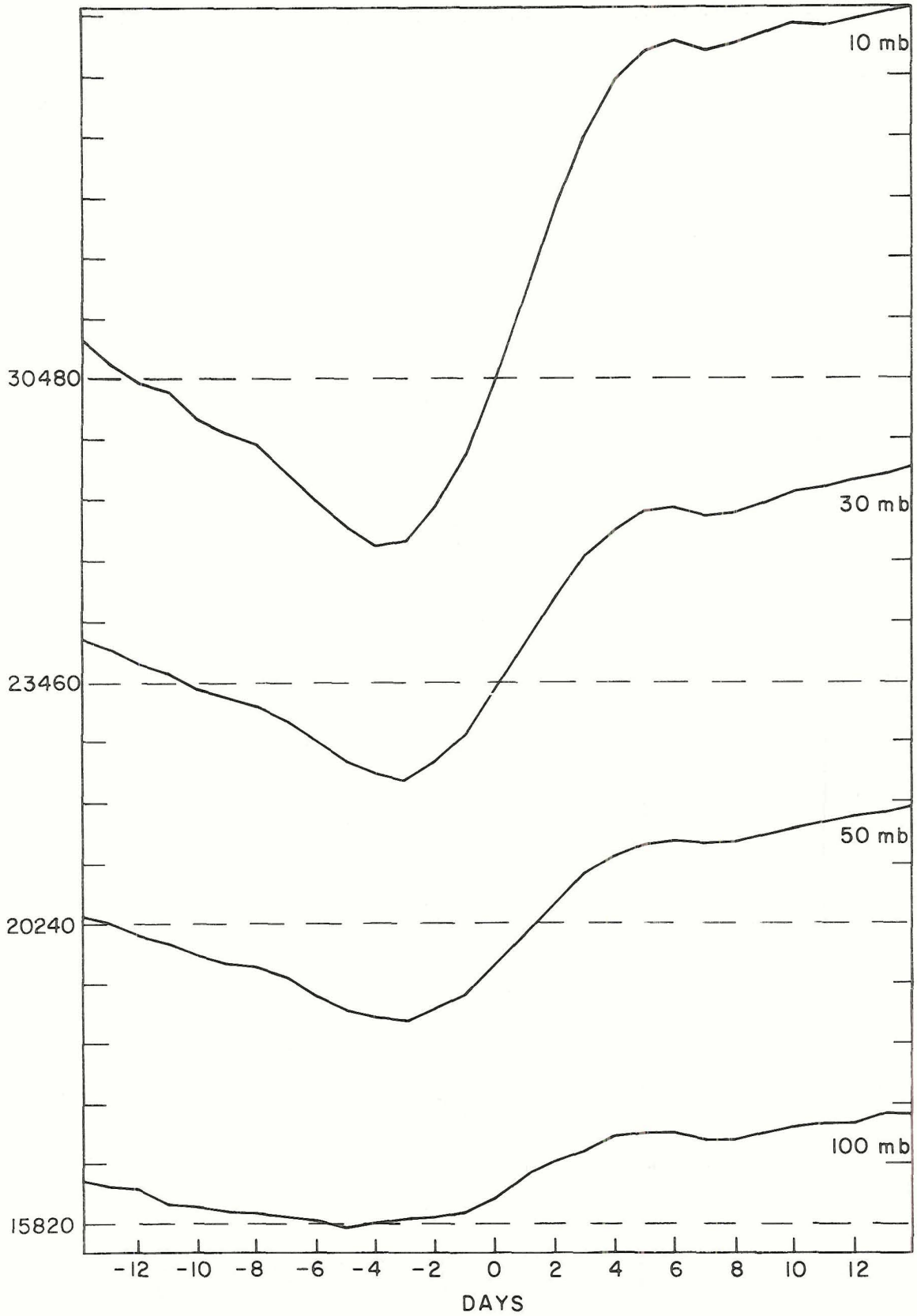


Figure 8(b). Superposed epoch averages of mean zonal height at  $50^{\circ}\text{N}$  at the 10,30,50,100 millibar levels surrounding key dates selected according to the Warming II criteria. Each vertical increment represents 20 gpm.

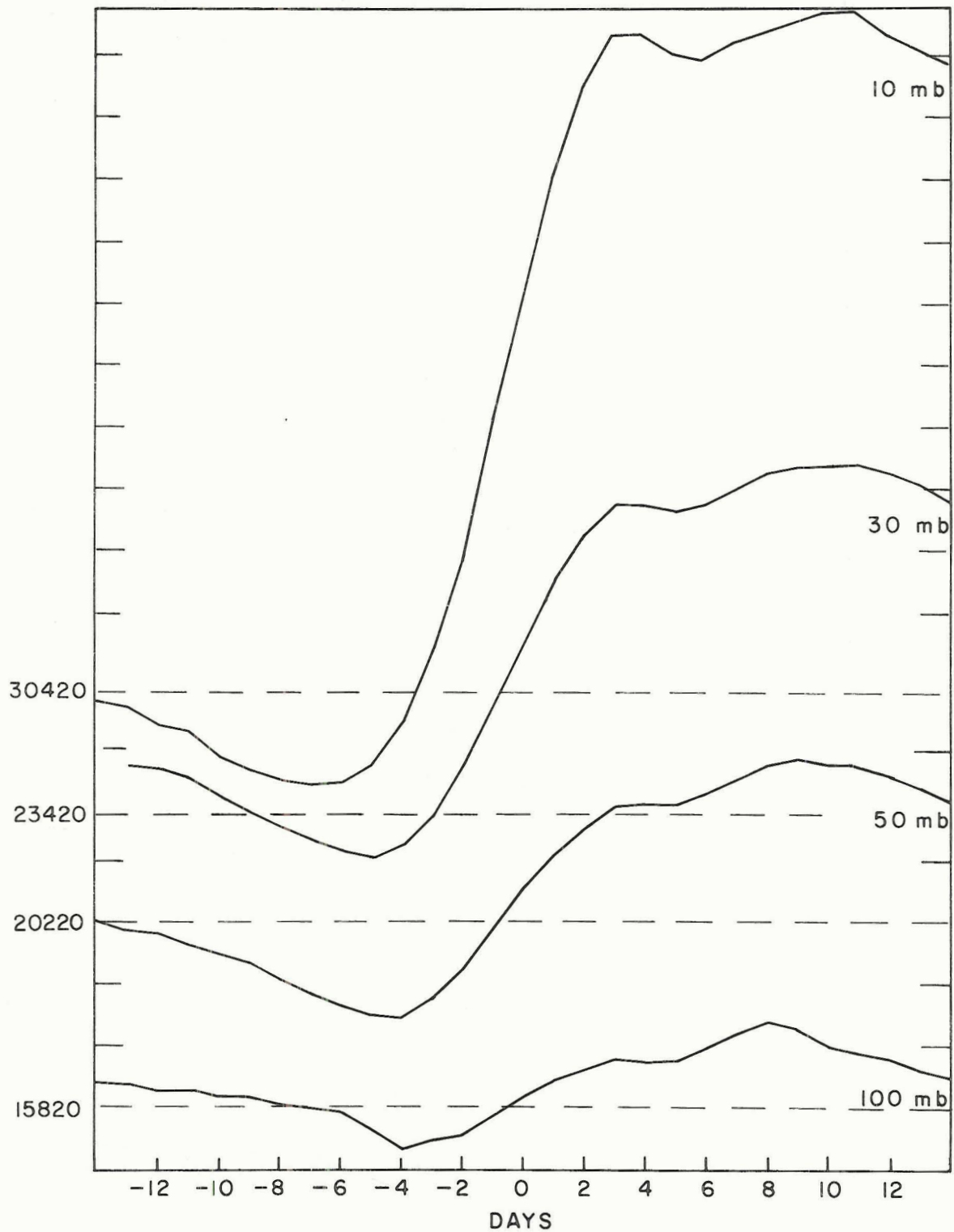


Figure 8(c). Superposed epoch averages of mean zonal height at 50°N at the 10, 30, 50, 100 millibar levels surrounding key dates selected according to the Warming III criteria. Each vertical increment represents 20 gpm.

described earlier, were used in an attempt to detect a tropospheric response. Using our data for the six seasons in which these two sets overlapped (1957-58 through 1962-63), we again took every possible nine-day sequence in each season and separated each into three three-day sequences. Key stratospheric warming events were determined in the following manner: The 30,640 meter contour mean latitude in the second three-day sequence must be greater than the mean of the first three-day sequence by two degrees of latitude or more, and similarly the mean of the third three-day sequence must also be greater than the second by two degrees or more. Key dates were again chosen as the fifth day (the middle day) of the nine-day sequence, and 52 such sequences in the six seasons met both criteria. Using the superposed epoch method, we determined the mean response of the tropospheric cold pool area surrounding these key dates. The mean values of the polar vortex mean latitude and the 500 millibar cold pool area are given in Figure 9. Note the shrinkage of the cold pool following the stratospheric warming, with the most significant shrinkage beginning about three days after the stratospheric warming. To test the statistical significance of this decrease in area we again used a simple rank sum test separately for each of the 52 sequences. We compared the area values of the  $D_{-5}$  through  $D_{-1}$  sequence with those of the  $D_8$  through  $D_{12}$  sequence. In 32 of the 52 epochs, the values in the latter sample were numerically less than the former sample at the 95 per cent significance level or better. In 40 of the cases, the numerical mean of the  $D_8$  through  $D_{12}$  sequence was less than the mean of the earlier sequence. This confirms a forcing upon the tropospheric cold pool

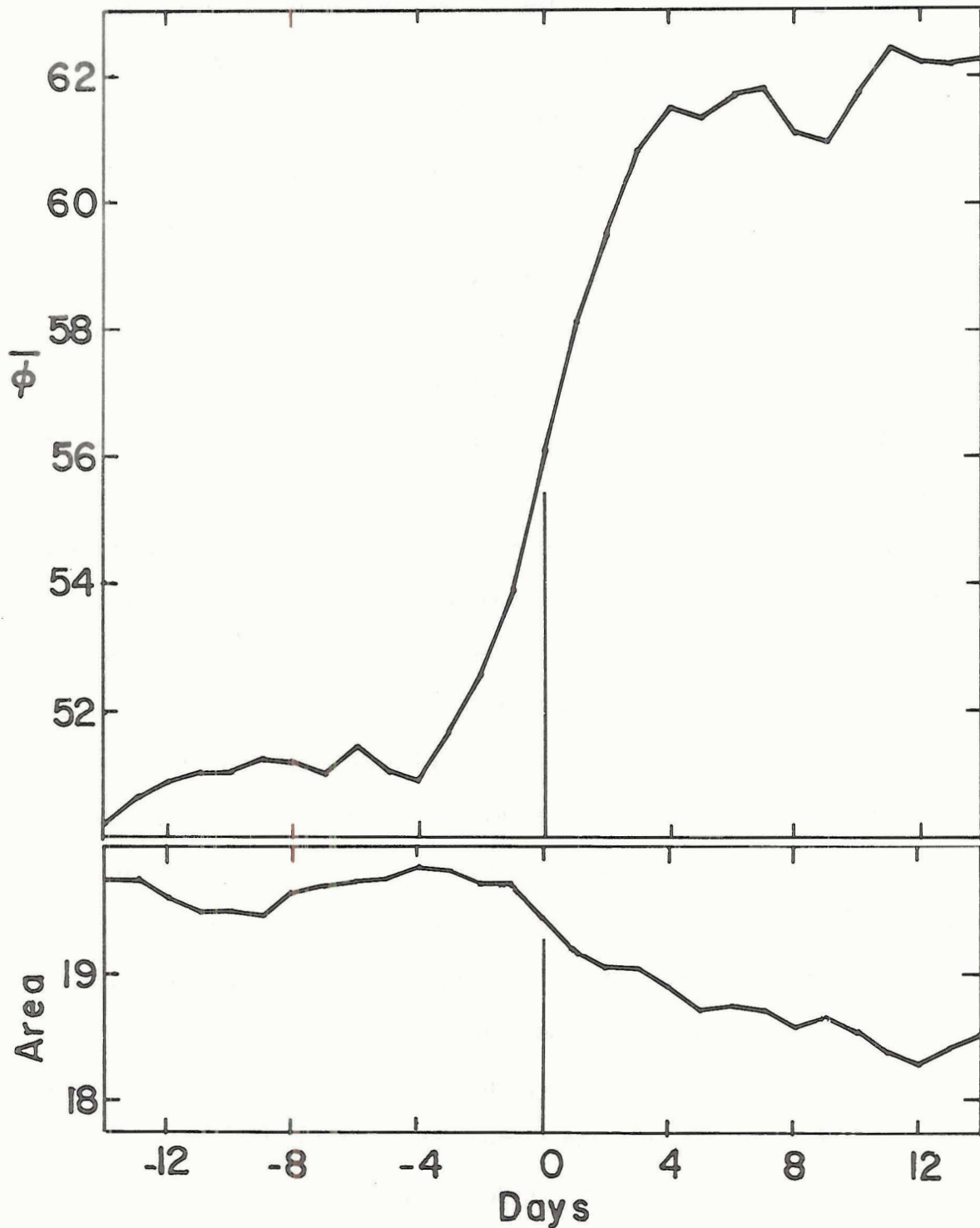


Figure 9. Superposed epoch averages of the 30,640 meter contour mean latitude ( $\bar{\phi}$ ) at 10 mb surrounding an increase in mean latitude of 4 degrees or more in 9 days (upper curve). The superposed epoch averages of the area of the cold air ( $T < 30^{\circ}\text{C}$ ) in arbitrary units surrounding such events are shown in the lower curve.

size by stratospheric warming events which are weaker than the events discussed by Reiter and Macdonald (1973).

It is probable that the reason that no tropospheric response to geomagnetic activity could be shown directly is that the intermediary action of the stratosphere tends to mask this effect over the time scales considered here. This would cause the tropospheric reaction to be spread over a greater length of time with respect to the Key Geomagnetic Date, and therefore it would be more difficult to detect in a statistical sense. The results presented in this section indicate that although the stratosphere responds more significantly to geomagnetic activity than does the troposphere, the resulting stratospheric warming may in turn be forced upon the troposphere.

## STABILITY OF THE POLAR VORTEX

Mahlman (1966) has shown that the stratospheric warming process depends directly on the magnitude of the horizontal eddy transport of heat. He has determined that a necessary condition for instability in the flow of the polar vortex is that the poleward gradient of the zonal mean potential vorticity on an isentropic surface should vanish, i.e.,

$$\frac{\partial \bar{P}}{\partial y_{\theta}} = 0$$

where  $\bar{P} = \frac{\partial \theta}{\partial P} (\zeta_{\theta} + f)$  averaged around a latitude circle. He also notes that from the calculations of  $\bar{P}$  it was evident that variations in the  $\frac{\partial \theta}{\partial P}$  term were more significant than variations in the other terms.

With this in mind we will examine the term  $\frac{\partial}{\partial y_{\theta}} \left( - \frac{\partial \theta}{\partial P} \right)$  to determine its value near a series of geomagnetic events. It has been suggested (Schuurmans, 1969; Manson, 1968) that the atmosphere may react to an influx of solar radiation when it is "nearly" unstable and that it may not react when its flow is stable. The twenty-two key Geomagnetic Dates from the 1964-65 through 1968-69 seasons which were preceded by at least nine non key dates were selected, and the  $\frac{\partial}{\partial y_{\theta}} \left( - \frac{\partial \theta}{\partial P} \right)$  term was calculated for the 30-10 millibar layer. Since pressure surfaces and potential temperature surfaces are both nearly horizontal at these levels, we will assume that  $\frac{\partial}{\partial y_{\theta}} \approx \frac{\partial}{\partial y_p}$ . The term

$-\frac{\partial\theta}{\partial P}$  was calculated every  $10^\circ$  latitude by  $10^\circ$  longitude in the latitude band  $50^\circ\text{N}$  to  $80^\circ\text{N}$  from NMC Octagonal Grid data. Daily zonal averages of  $-\frac{\partial\theta}{\partial P}$  were calculated and the meridional gradients of these values were determined for the three latitude bands:  $50^\circ$ - $60^\circ\text{N}$ ,  $60^\circ$ - $70^\circ\text{N}$ ,  $70^\circ$ - $80^\circ\text{N}$ .

Proceeding with the hypothesis that the polar vortex' reaction to precipitating solar corpuscular radiation will be stronger when it is nearly unstable than when it is not, we will examine the meridional gradient of potential vorticity near a Key Geomagnetic Date. When the three calculated gradients are of different sign, or one of the gradient values falls within the range

$$-0.01 \text{ }^\circ\text{K mb}^{-1} \text{ }^\circ\text{lat}^{-1} < \frac{\partial}{\partial y} \left( -\frac{\partial\theta}{\partial P} \right) < 0.01 \text{ }^\circ\text{K mb}^{-1} \text{ }^\circ\text{lat}^{-1}$$

for either the day of a geomagnetic event or the day immediately preceding the key date or the day immediately following it, we will label the situation nearly unstable. When the gradients do not meet these above mentioned criteria, we will label the situation stable. Of the twenty-two key dates in the five seasons, sixteen of the events possessed a nearly unstable polar vortex and the remaining six were stable.

The mean value of the 30,640 meter contour daily mean latitude as well as its standard deviation for the five days preceding each Key Geomagnetic Date were determined. The mean value of these parameters from  $D_5$  through  $D_9$  were also calculated. Table 2 shows the results of these computations. In Column 1 we note a mean increase in the 30,640 meter mean latitude after a key geomagnetic date when the flow is

nearly unstable, and we also note an increase in standard deviation following such dates. Observe that in Column 2 of Table 2 for key geomagnetic dates with stable flow the increase in mean latitude is less than that of Column 1 while the change in standard deviation in both columns is comparable. Appendix C shows a tabulation of all individual daily values of mean latitude and standard deviation which were used in computing the values in Table 2. A rank sum test applied to each of the 16 nearly unstable events shows that this increase in mean latitude is statistically significant at the 95 per cent level in nine cases. The increase in standard deviation achieved the same level of significance in only five cases, however.

A valid criticism of this approach is that since we are estimating vortex instability, the observed warming around the vortex edge might have occurred due to this instability regardless of a solar influence. To overcome this shortcoming, sixteen "complementary key dates" were randomly selected with the following restrictions: The flow on these dates met the same criteria as that of the nearly unstable situation; the dates were not associated with a geomagnetic disturbance; and one date with exactly the same day and month as each of the dates of the nearly unstable flow-geomagnetic key date situation was chosen. This latter criterion had the effect of cancelling any seasonal bias introduced into the other sample. In this way the mean reaction of the polar vortex edge when the vortex is "nearly unstable" for the occasions of an active sun and those of a quiet sun can be compared. These computed mean values are shown in the third column of Table 2. Notice that on the average a cooling as well as a decrease in the meridional component of the geostrophic flow near the edge of the

polar vortex is implied. Oddly enough, an increase in mean latitude and an increase in standard deviation of this contour occurs in seven of the sixteen cases. This is nearly what one would expect for a random fluctuation.

Apparently the polar vortex reacts to solar variability to a greater degree when the flow is nearly unstable as opposed to when the flow is more stable. An equivalent reaction for nearly unstable flow without a sudden increase in geomagnetic activity is not noticed.

TABLE 2

A comparison of mean values of the 10 millibar 30,640 meter contour mean latitude and standard deviation for specific five day periods preceding and following certain key events.

	Column 1	Column 2	Column 3
	Key geomagnetic dates, flow nearly unstable.	Key geomagnetic dates, flow stable.	Non-key geomagnetic dates, flow nearly unstable.
Mean value of D <sub>-5</sub> through D <sub>-1</sub> mean latitude.	51.12	50.09	50.32
Mean value of D <sub>5</sub> through D <sub>9</sub> mean latitude.	53.02	50.51	49.95
Mean value of D <sub>-5</sub> through D <sub>-1</sub> standard deviation.	13.82	13.83	13.89
Mean value of D <sub>5</sub> through D <sub>9</sub> standard deviation.	14.65	14.77	12.91
Number of cases.	16	6	16

## POSSIBLE MECHANISMS

Several mechanisms have been suggested. These take the relatively small amount of energy associated with solar variability and trigger reactions in the stratosphere which are associated with comparatively large amounts of energy. We will present some of them here, and we will discuss the implications of our findings upon these schemes.

### 1. The Polar Vortex Center.

Before determining the mechanism which brings about the shrinkage of the polar vortex discussed in the preceding section, it is important to examine the fluctuations of the vortex center surrounding such warming events. If the center contour at 10 millibars shows a marked increase at the time that the edge of the vortex shrinks, a mechanism of large scale subsidence would suggest itself. A schematic indication of a typical event of this type, if it exists, is shown in Figure 10. On the other hand, if the center contour remained essentially at the same value or became numerically less during shrinkage, a steepening of the contour gradient near the edge of the vortex would be associated with a contraction of the vortex edge. Some mechanism, such as mass importation or warming only along a rather narrow belt, would be indicated. Figure 11 shows a schematic interpretation of an event of this type.

We examined the fluctuations in central contour value during a 29 day epoch surrounding a contraction of the vortex edge. As before

we used the criterion in which the mean latitude of the 30,640 m contour at 10 millibars increased by four degrees or more in nine days using the method with the three day means described in the previous section. The superposed epoch method was employed with the key date again chosen as the middle day of such nine day sequences. In the twelve seasons for which we have 10 millibar data, 76 nine day sequences met the criterion. The means of the 30,640 m mean latitude values for these events are shown in Figure 12. The means of the central contour value at 10 millibars during these epochs are also shown in Figure 12. Note that no increase in height of this pressure surface is even remotely suggested; in fact a mean decrease of about 20 meters is implied. On the basis of these results we can rule out any mechanism which promotes large scale subsidence over the pole as being responsible for a shrinkage of the polar vortex. We are forced to rely on a mechanism which causes a steepening of the contour gradient (on a constant pressure surface) near the edge of the polar vortex to bring about the observed contraction.

## 2. Direct Absorption.

One possibility of warming the polar vortex edge at 10 millibars would be through collisional excitation and ionization of the atmospheric molecules during the geomagnetic storm, i.e., direct absorption of energy. Certainly the fact that auroras occur along a latitude belt which is near the polar vortex edge gives impetus to an investigation of this possibility. We will present some calculations showing that this mechanism cannot supply the required energy to bring about the observed contraction.

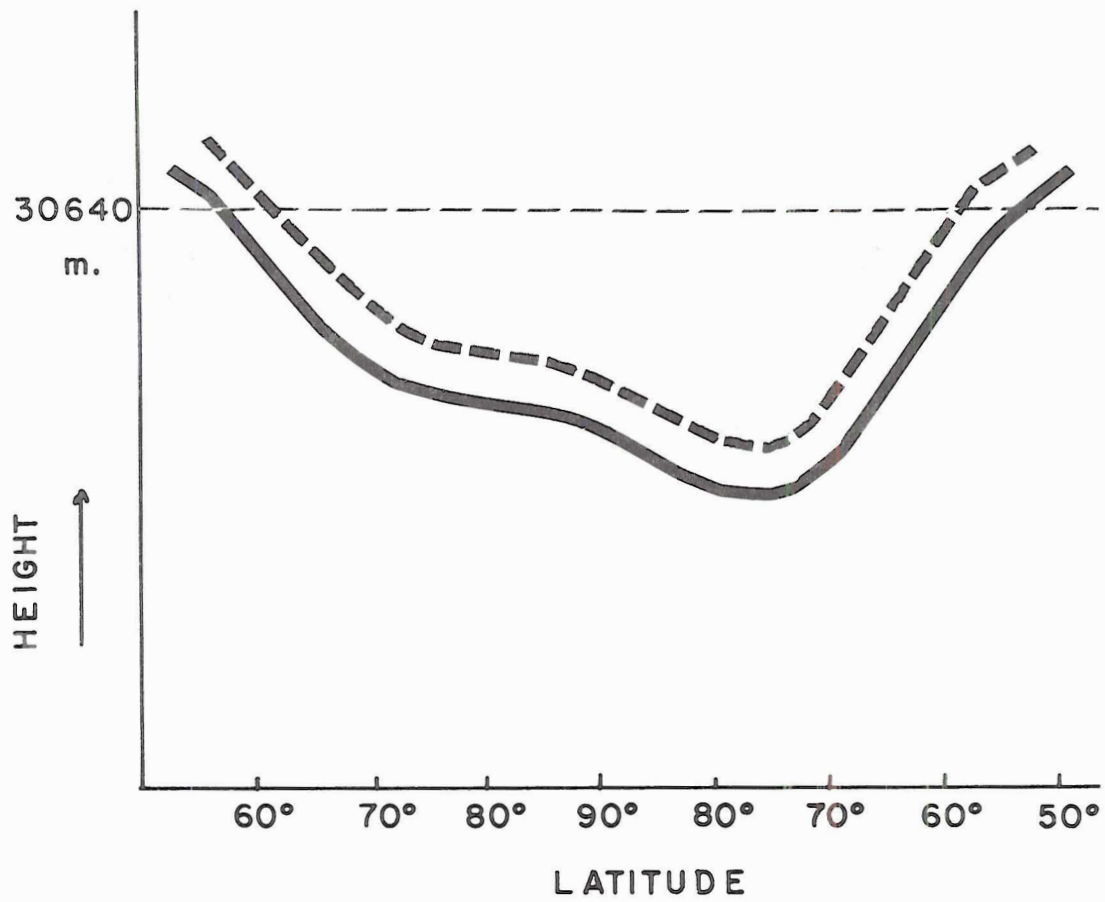


Figure 10. Meridional cross section (over the pole) of the 10 millibar surface surrounding an increase in mean latitude (shrinkage of the polar vortex) of the 30,640 meter contour, if it is associated with large scale warming or subsidence. The solid line represents the 10 millibar heights preceding the shrinkage and the dashed curve represents height values following the shrinkage.

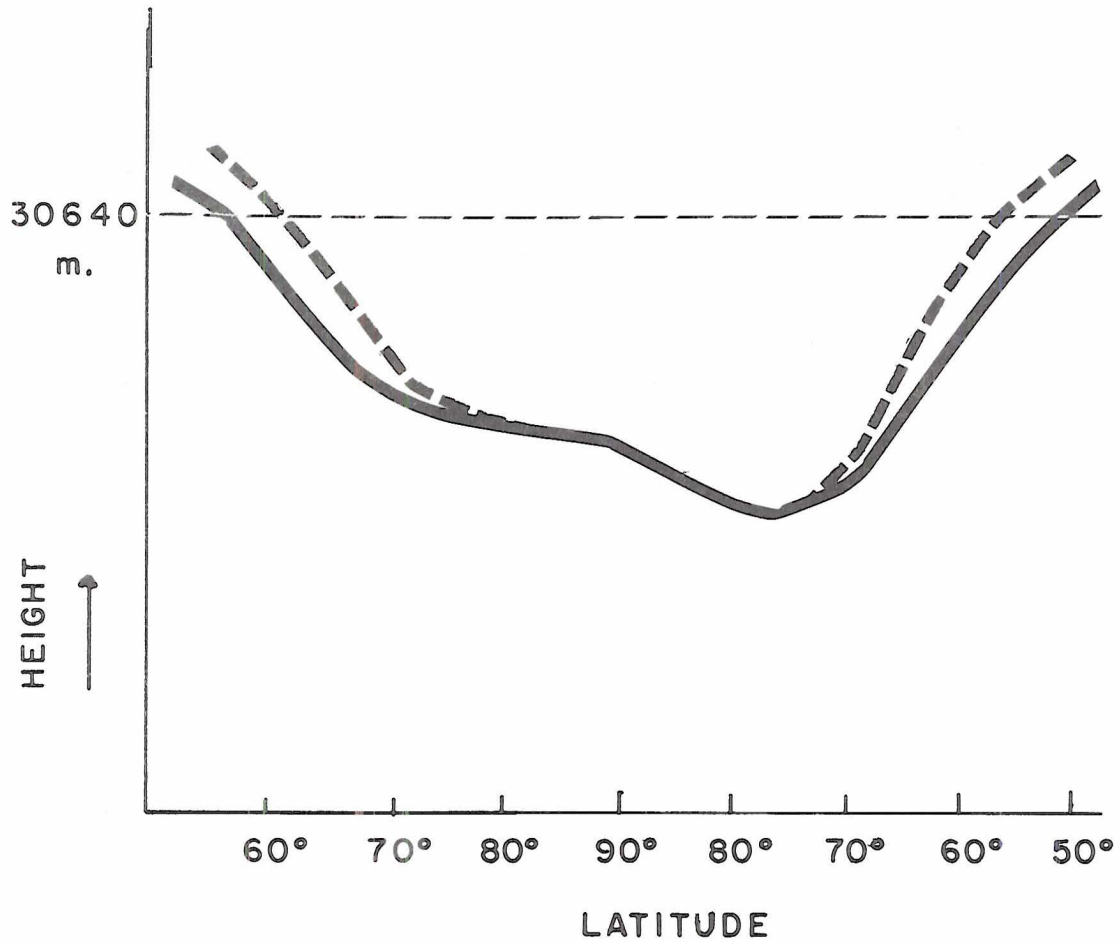


Figure 11. Meridional cross section (over the pole) of the 10 millibar surface surrounding an increase in mean latitude (shrinkage of the polar vortex) of the 30,640 meter contour, if it is associated with a steepening of the contour gradient along the vortex edge. The solid line represents the 10 millibar heights preceding the shrinkage, and the dashed curve represents height values following it.

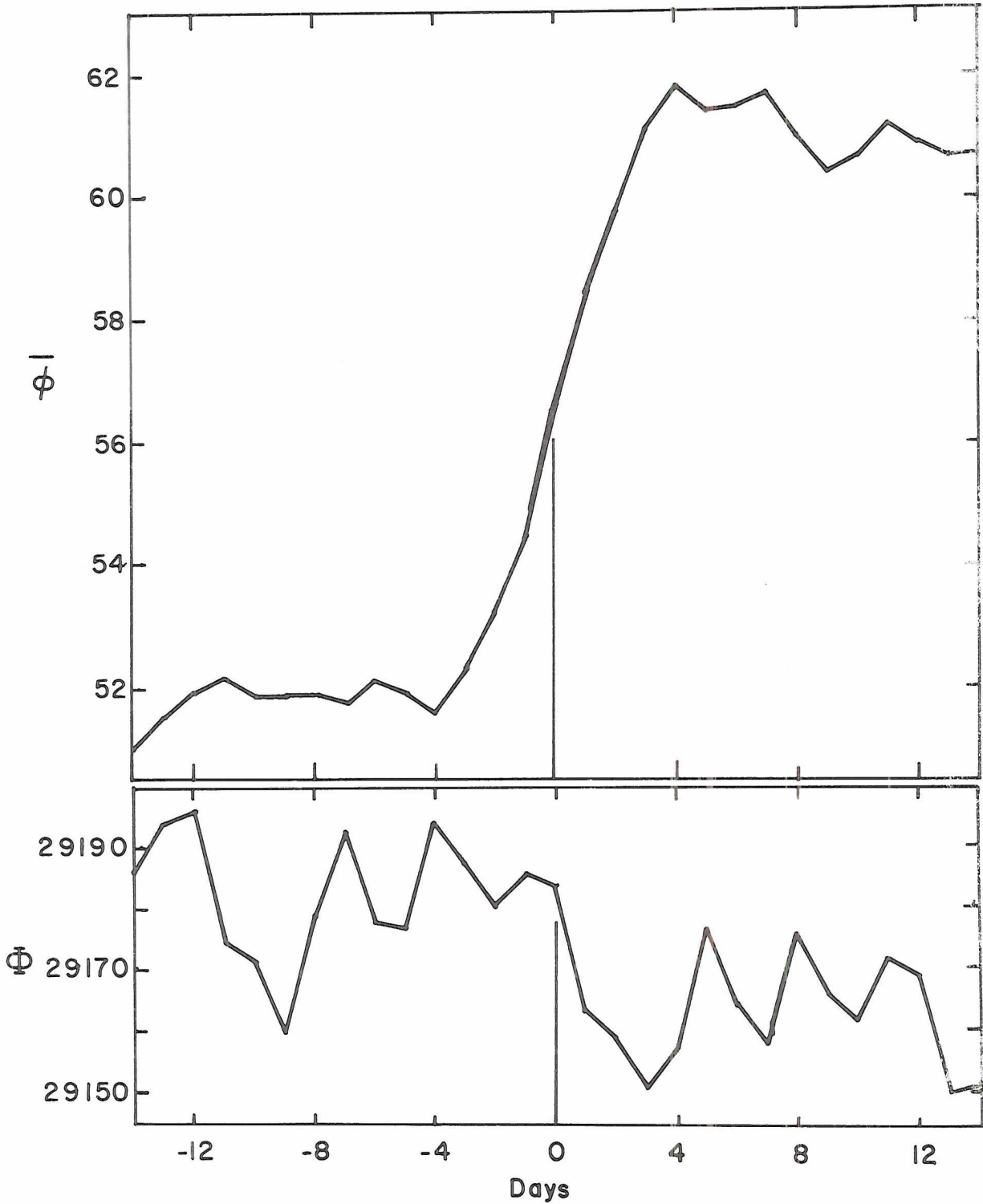


Figure 12. Superposed epoch averages of the 30,640 meter contour mean latitude ( $\bar{\phi}$ ) at 10 mb surrounding an increase in mean latitude of four degrees or more in 9 days (upper curve). The superposed epoch averages of the value (in meters) of the polar vortex central contour at 10 mb are shown on the lower curve.

According to Matsushita and Campbell, (1967) we can assume that the auroral absorption takes place primarily in a band  $10^\circ$  of latitude wide, averaging 5000 km in length in both hemispheres. The rate of dissipation due to auroral processes during a magnetic storm is about  $10^{17}$  to  $10^{18}$  erg sec<sup>-1</sup> (Knecht, 1972). The area of one of these bands is about  $5.6 \times 10^{16}$  cm<sup>2</sup>, and we will assume that  $10^{18}$  erg sec<sup>-1</sup> are absorbed over one of these bands during a magnetic storm. A cursory examination of the contour gradient at 10 millibars near the polar vortex edge in midwinter yields a mean contour gradient of about -80 m (degree latitude)<sup>-1</sup>, shown schematically in Figure 13. If we assume uniform heating of a 10 degree latitude band (from 50°N to 60°N) only, a four degree increase in mean latitude of the 30,640 m contour line would require a uniform 320 meter increase in height of the 10 millibar surface over this latitude band. If this increase is due totally to heating in, say, the 30 to 10 millibar layer, the calculations shown in Appendix A indicate a required mean warming of about 10°C in this layer. Also in Appendix A, calculations of energy required to carry on this heating compared with energy available from a  $10^4$  sec geomagnetic initial phase show that simple absorption and redistribution of the auroral energy could not possibly account for the noted heating.

### 3. Other Approaches.

Cobb (1967) investigates the possibility that enhanced solar corpuscular radiation incident upon the earth following a solar flare alters the air-earth electrical current and causes a global increase in the total amount of thunderstorm activity. He cites the classical

hypothesis of the global concept of the atmospheric electrical current which views the earth and the ionosphere (50-75 km) as highly conducting concentric layers separated by an imperfect insulating lower atmosphere. As described by Cobb (op. cit.) this so-called "Wilson Circuit" can be summarized as follows: Over fair weather areas of the earth, there is a downward transfer of positive charge which tends to reduce the positive potential of the ionosphere and neutralize the negative charge on the earth. Over stormy areas of the globe, on the other hand, positive charge is transferred upward at a rate proportional to the total thunderstorm activity and of sufficient quantity to balance the fair-weather downward transfer of positive charge. Cole and Pierce (1965) calculated that 90% of the earth-ionosphere columnar resistance lies below 2.4 km, and changes above this level do not appreciably alter the total resistance for the vertical conduction current. Both Cobb (1967) and Reiter (1969) have noted an increase in the vertical potential gradient as well as the fair weather current from one to four days following a solar flare event. Such increases are generally 10% over the "quiet" mean values, but some have been noted as high as 60% for highly disturbed cases. Precisely how the flux of solar corpuscular radiation could enhance these values is not well known. However, if such an enhancement produced an increase in global total thunderstorm activity, its implication for the modification of tropospheric weather and climate would be significant. Measurements of global total thunderstorm occurrence and intensity as well as a greater understanding of the ionosphere-earth electric circuit interaction with solar corpuscular radiation will be needed to examine the feasibility of this mechanism.

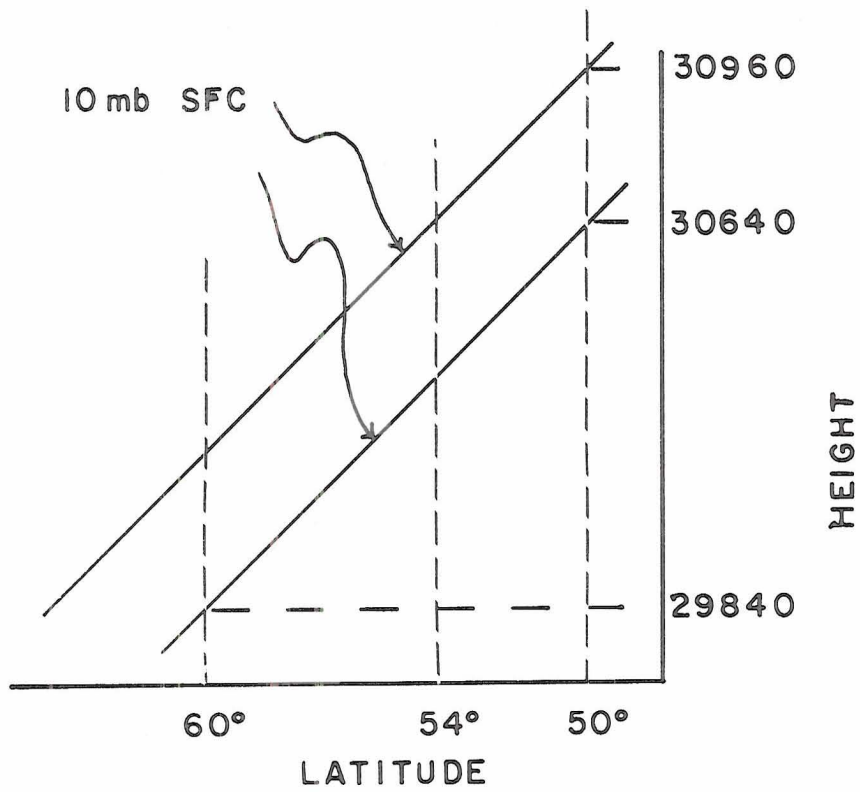


Figure 13. A schematic diagram of two 10 millibar surfaces with latitudinal height gradients of -80 meters per degree latitude.

Roberts and Olson (1973a,b) have suggested that the Bremsstrahlung radiation which precipitates into the atmosphere after a solar flare may reach the nearly saturated air near the tropopause, act as ice nucleants and create a thin cirrus deck. If not pre-existing, such a cloud pattern would alter the radiative infrared balance in the atmosphere and bring about an alteration in tropospheric weather patterns. At the cold temperatures usually noted near the tropopause,  $-40^{\circ}\text{C}$  and colder, however, the atmosphere apparently has an overabundance of ice nuclei. Mason (1971) notes that ice nuclei concentrations near the tropopause are probably as high as those near the surface. Formation of cirrus would depend on the saturation of air rather than the availability of ice nuclei active at those temperatures. It would therefore seem improbable that the addition of any ice nuclei at these levels in the atmosphere would have any effect. However, measurements of ice nuclei counts at high elevations especially over oceans are not abundant. Nevertheless, such measurements of ice nuclei, along with an estimation from satellites of changes in cirrus shield, might be made in order to further investigate this hypothesis.

Schuermans (1969) proposes that in entering the lower stratosphere, protons dislodge electrons by numerous collisions with air molecules. Some of these electrons have energies sufficient to dissociate water vapor. He suggests that with water vapor available near the tropopause, it becomes much more likely that this level is the seat of the initial atmospheric reaction to solar variability. These dissociated water molecules act to remove ozone from the lower stratosphere, upsetting the radiational balance, and bringing about a cooling near the tropopause. Such a cooling, which he calculated to be significant,

may then act as a modifier of tropospheric phenomena. The precipitation of high energy solar corpuscular radiation (protons with energies between 300 and 1000 MeV) to levels in the lower stratosphere is a crucial factor in Schuurmans' mechanism. However, he uses extrapolations of other researchers' formulas to estimate the flux of these particles to this level, and it is not clear that these formulas are applicable for this purpose. Accurate measurements and calculations of these fluxes in the lower stratosphere are clearly needed.

#### 4. Discussion.

Wilcox et al. (1973) produce a figure which shows their vorticity area index values during a superposed epoch analysis surrounding sector passage dates at stratospheric levels. (See Figure 14.) They neglect to comment on the apparently downward propagating minimum value of their index which occurs about three days prior to the key date. Although sector boundary passage is not completely understood, it appears that stratospheric flow is reacting to such an event.

Labitzke (1972a,b) indicates that stratospheric and mesospheric temperature patterns tend to be related. She notes a gradual warming of the stratopause coincident with a cooling of lower stratospheric and upper mesospheric layers. When the vortex breaks down, the stratopause cools and the upper mesosphere and lower stratosphere appear to warm. A mechanism related to solar variability which can trigger such an event may prove to link that variability to effects in the stratosphere.

Of course the warming we observe in the stratosphere may be a manifestation of events taking place in the troposphere. Mechanisms

## HEMISPHERIC VORTICITY AREA vs SECTOR BOUNDARIES

1964 - 1970  
 NOVEMBER - MARCH  
 ALL LONGITUDES

VORTICITY DISCRIMINATOR =  $20 \times 10^{-5} \text{ sec}^{-1}$

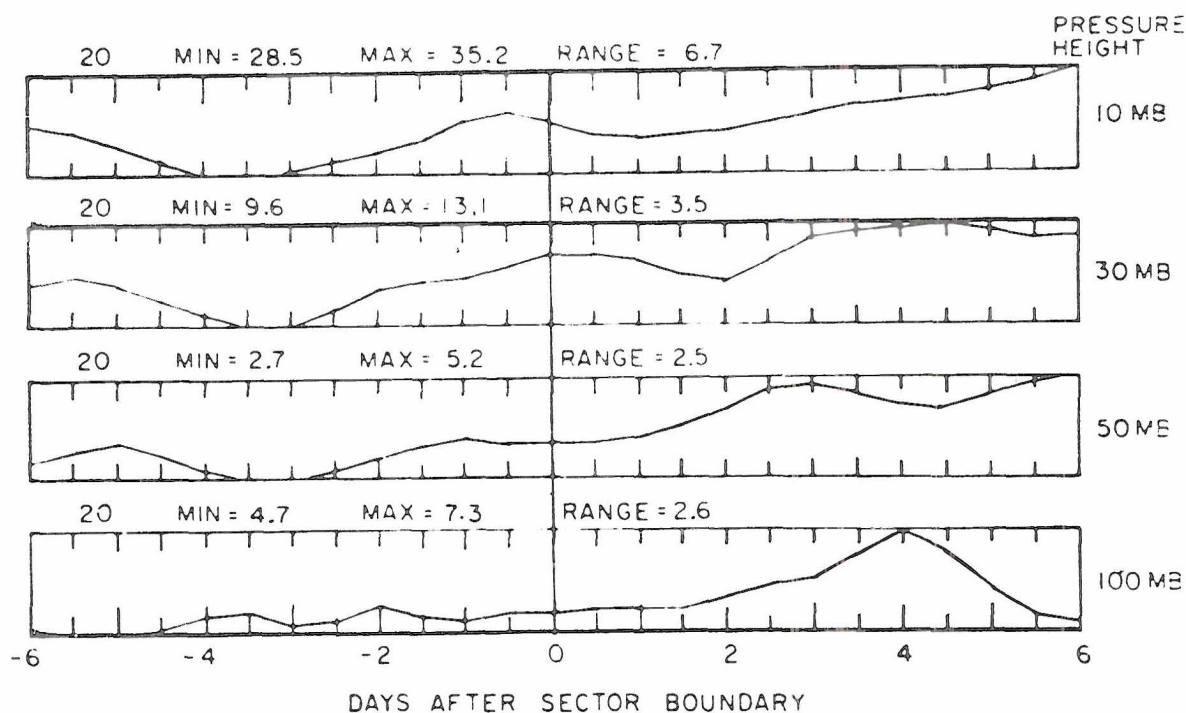


Figure 14. Superposed epoch analyses of average response of hemispheric vorticity area to passing of 54 sector boundaries in the northern hemisphere north of  $20^{\circ}\text{N}$  latitude in which the vorticity exceeded a value of  $20 \times 10^{-5} \text{ sec}^{-1}$  are included. The results are shown for pressure levels of 10 mb, 30 mb, 50 mb, and 100 mb. Each graph includes the maximum and minimum values of the vorticity area within the range  $\pm 6$  days from sector boundary passage. At the top of each graph is listed the vorticity discriminator in units of  $10^{-5} \text{ sec}^{-1}$ , and the minimum, maximum, and range of the vorticity area are in units of  $10^5 \text{ km}^2$ . (From Wilcox, et al., 1973).

which have been proposed by others which deal with a tropospheric reaction along with a resultant upward transfer of these effects may be the link between solar variability and our results. In addition, no one can rule out the possibility that different mechanisms are operating at these different levels, and the forcing between the layers is of minor importance.

## CONCLUSION

Our statistical results seem to indicate that the stratospheric flow is reacting to solar variability. The relation between this solar variability and the observed warming near the edge of the polar night vortex and the increase in the meridional component of stratospheric flow at 10 millibars is difficult to deny. The magnitude of the reaction of the flow seems to depend upon the initial condition of vortex stability. Warmings perceived at the middle levels of the stratosphere appear to be propagated downward. Even though our sample sizes are not large and our observations are only statistical, a mechanism which promotes a reaction of stratospheric flow to solar variability demands to be discovered.

## REFERENCES

- Brooks, C. E. P., 1923: Variations in the level of central African Lakes. Geophys. Mem., 20, London (Met. Office).
- Cobb, W. E., 1967: Evidence of a solar influence on the atmospheric electric elements at Mauna Loa Observatory. Mon. Wea. Rev., 95, 905-911.
- Cole, R. K., Jr., and E. T. Pierce, 1965: Electrification in the Earth's atmosphere for altitudes between 0 and 100 kilometers. J. Geophys. Res., 70, 2735-2749.
- Jagannathan, P., and H. N. Bhalme, 1973: Changes in the pattern of distribution of southwest monsoon rainfall over India associated with sunspots. Mon. Wea. Rev., 101, 691-700.
- Knecht, D. J., 1972: The geomagnetic field, a revision of Chapter 11, Handbook of Geophysics and Space Environments. Air Force Surveys in Geophysics, No. 246., AFCRL-72-0570. 120 pp.
- Labitzke, K., 1964: On the mutual relation between stratosphere and troposphere during periods of stratospheric warmings in winter. J. Appl. Met., 4, 91-99.
- \_\_\_\_\_, 1972a: Temperature changes in the mesosphere and stratosphere connected with circulation changes in winter. J. Atmos. Sci., 29, 756-766.
- \_\_\_\_\_, 1972b: The interaction between stratosphere and mesosphere in winter. J. Atmos. Sci., 29, 1395-1399.
- Lamb, H. H., 1972: Climate Present, Past and Future. Methuen & Co. London.
- London, J., I. Ruff, and L. J. Tick, 1959: The relationship between geomagnetic variations and the circulation at 10 mb. J. Geophys. Res., 64, 1827-1833.
- Macdonald, N. J., and W. O. Roberts, 1960: Further evidence of a solar corpuscular influence on large-scale circulation at 300 mb. J. Geophys. Res., 65, 529-534.
- Mahlman, J. D., 1966: Atmospheric general circulation and transport of radioactive debris. Ph.D. Dissertation, Colorado State University, Fort Collins.

- Manson, A. H., 1969: The effect of solar corpuscular radiation on the 1963 final spring warming in the Antarctic. J. Atmos. Sci., 26, 587-593
- Mason, B. J., 1971: The Physics of Clouds. Clarendon Press, Oxford. 671 pp.
- Reiter, E. R., 1963: Jet Stream Meteorology. University of Chicago Press. 513 pp.
- \_\_\_\_\_, 1971: Atmospheric Transport Processes Part 2: Chemical Tracers. USAEC Division of Technical Information Extension, TID-25314. 382 pp.
- \_\_\_\_\_, and B. C. Macdonald, 1973: Quasi-biennial variations in the wintertime circulation of high latitudes. Arch. Met. Geophys. Biokl. Ser. A, 22, 145-167.
- Reiter, R., 1969: Solar flares and their impact on potential gradient and air-earth current characteristics at high mountain stations. Pure Appl. Geophys., 72, 259-267.
- Roberts, W. O., 1973: Relationships between solar activity and climate change. Proceedings, Symposium on the Possible Relationship between Solar Activity and Meteorological Phenomena (in press).
- \_\_\_\_\_, and R. H. Olson, 1973a: Geomagnetic storms and wintertime 300 millibar trough development in the North Pacific-North America area. J. Atmos. Sci., 30, 135-140.
- \_\_\_\_\_, and R. H. Olson, 1973b: New evidence for effects of variable solar corpuscular emission on the weather. Rev. of Geophys. and Space Phys., 11, 731-740.
- Schuurmans, C. J. E., 1969: The Influence of Solar Flares on the Tropospheric Circulation. Koninklijk Nederlands Meteorologisch Instituut Mededelingen en Verhandelingen. 123 pp.
- Shapeley, A. H. and W. J. G. Beynon, 1965: Winter anomaly in ionospheric absorption and stratospheric warmings. Nature, 206, 1242-1243.
- Shapiro, R., 1956: Further evidence of a solar-weather effect. J. Meteor., 13, 335-340.
- \_\_\_\_\_, 1959: A comparison of the response of the North American and European surface pressure distributions to large geomagnetic disturbances. J. Meteor., 16, 569-572.
- \_\_\_\_\_, 1972: A test of an apparent response of the lower atmosphere to solar corpuscular radiation. J. Atmos. Sci., 29, 1213-1216.

- Shapiro, R., and H. L. Stolov, 1970: Surface pressure variations in polar regions. J. Atmos. Sci., 27, 1021-1026.
- Sinno, K., and M. Higashimura, 1969: Development of ionospheric absorption associated with stratospheric warmings in 1958 and 1963. J. Atmos. Terr. Phys., 31, 1353-1357.
- Stolov, H. L. and R. Shapiro, 1969: Further investigations of alleged tropospheric responses to chromospheric flares. J. Atmos. Sci., 26, 1355-1359.
- Ward, F. W., Jr., 1960: Atmospheric temperatures and solar activity--100 mb in the northern hemisphere auroral zone. J. Meteor., 17, 130-134.
- Wilcox, J. M., and N. F. Ness, 1965: Quasi-stationary corotating structure in the interplanetary medium. J. Geophys. Res., 70, 5793-5805.
- Wilcox, J. M., P. H. Scherrer, L. Svalgaard, W. O. Roberts, R. H. Olson, and R. L. Jenne, 1973: Influence of Solar Magnetic Structure on Terrestrial Atmospheric Vorticity. Stanford University Institute for Plasma Research. Report No. 530, 31 pp.
- Willett, H. C., 1968: Remarks on the seasonal change of temperature and of ozone in the Arctic and the Antarctic stratospheres. J. Atmos. Sci., 25, 341-360.
- Wollin, G., G. J. Kulka, D. B. Ericson, W. B. F. Ryan, and J. Wollin, 1973: Magnetic intensity and climatic changes, 1925-1970. Nature, 242, 34-347.

APPENDICES

## APPENDIX A

1. Assume a mean temperature of 218°K [-55°C] in the 30 mb-10 mb layer.
2. Given the formula from the Smithsonian Tables:

$$\Delta\phi = 67.442 (273.16 + t'_{mv}) \log_{10} \frac{P_1}{P_2}$$

where:  $\Delta\phi$  = thickness of the layer (gpm)

$t'_{mv}$  = mean adjusted virtual temperature of  
the layer (°C)

$P_1$  = pressure at the base of the layer

$P_2$  = pressure at the top of the layer

3. Using this formula with the values given in (1.) above

$$\Delta\phi = 7020 \text{ gpm}$$

4. If we increase the thickness of this layer by 320 gpm and reapply the equation in (2.),

$$t'_{mv} = -45^\circ\text{C}$$

5. Therefore, corresponding to an increase of 320 gpm in the 30 mb-10 mb layer, the mean virtual temperature must increase by 10°C.
6. From the text, we had assumed that the area of the latitude band in which auroral energy is absorbed is  $5.6 \times 10^{16} \text{ cm}^2$ .

7. The mass of air in the 30 mb-10 mb layer over this band is  
 $(20 \text{ g cm}^{-2}) (5.6 \times 10^{16} \text{ cm}^2) = 1.1 \times 10^{18} \text{ g}.$
8. Given the specific heat of air  $c_p = 10 \text{ erg g}^{-1} \text{ }^\circ\text{K}^{-1}.$
9. The energy required to bring about this observed warming = (total mass to be heated) (specific heat of the mass) (change in temperature required), or from (7.), (8.), and (5.) above. Energy required =  $(1.1 \times 10^{18} \text{ g}) (10^6 \text{ erg g}^{-1} \text{ }^\circ\text{K}^{-1}) (10^\circ\text{K}) = 1.1 \times 10^{25} \text{ erg}.$
10. From Matsushita and Campbell, assume that the energy of an auroral absorption is  $10^{18} \text{ erg sec}^{-1}.$
11. Assume that this strong absorption lasts  $\sim 3$  hours or  $10^4 \text{ sec}.$
12. Then the total energy involved in the aurora is

$$(10^{18} \text{ erg sec}^{-1}) (10^4 \text{ sec}) = 10^{22} \text{ erg}.$$

13. Comparing the results from (9.) and (12.), note that the energy involved in an aurora is much less than is required to produce the noted heating.

## APPENDIX B

Assume a four degree increase in mean latitude of the 30,640 m contour at 10 mb, and assume that this is brought about by the 10°K warming in the 30 mb-10 mb layer noted in Appendix A.

Differentiating Poisson's equation and holding  $d\theta = 0$  where  $P = 20$  mb,  $T = 223^\circ\text{K}$ , let  $dT = + 10^\circ\text{K}$

$$d\theta = dT \left( \frac{1000}{P} \right)^K - KT(1000)^K P^{-K-1} dp$$

$$\text{then } dp = 3.1 \text{ mb}$$

Using the hydrostatic approximation, this corresponds to a change of about 1070 gpm.

Therefore a parcel of air which sinks adiabatically from the 20 mb level,  $T = 223^\circ\text{K}$ , and warms  $10^\circ\text{K}$  must experience a change in geopotential of  $\sim 1070$  gpm.

If this change in geopotential is experienced over a period of nine days ( $7.78 \times 10^5$  sec), then the mean vertical motion which accounts for this warming is about  $-.14 \text{ cm sec}^{-1}$ .

## APPENDIX Ca

Daily 30,640 m contour (at 10 mb) mean latitude,  $\bar{\phi}$ , and standard deviation,  $\sigma$ , for selected dates preceding and following the occurrence of a geomagnetic key date when the polar vortex flow was nearly unstable. The mean values of each selected set of five days are also given.

Date		12/16/64	1/22/65	2/7/65	2/21/65	1/20/66	2/23/66	3/14/66	11/28/66
$\bar{\phi}$	D <sub>-5</sub>	46.92	52.67	51.92	54.08	43.83	59.58	49.75	54.50
	D <sub>-4</sub>	48.25	49.75	52.75	53.67	44.25	63.25	49.08	54.33
	D <sub>-3</sub>	47.33	51.25	49.92	55.17	43.83	63.00	48.08	53.00
	D <sub>-2</sub>	47.67	49.92	52.33	53.83	45.75	62.50	48.75	53.67
	D <sub>-1</sub>	47.33	50.50	51.50	54.58	46.42	63.17	48.17	51.25
D <sub>-5</sub> to D <sub>-1</sub> mean $\bar{\phi}$		47.50	50.82	51.68	54.27	44.82	62.30	48.77	53.35
$\bar{\phi}$	D <sub>5</sub>	47.33	48.17	56.00	56.25	49.00	75.10	50.00	48.67
	D <sub>6</sub>	46.33	46.83	55.25	56.50	49.67	72.62	51.33	47.83
	D <sub>7</sub>	49.42	47.75	54.83	56.50	49.92	71.00	50.42	49.75
	D <sub>8</sub>	49.33	49.33	54.75	56.00	50.92	69.12	53.08	47.83
	D <sub>9</sub>	49.25	51.00	54.08	56.42	50.42	73.42	53.67	46.42
D <sub>5</sub> to D <sub>9</sub> mean $\bar{\phi}$		48.33	48.62	54.98	56.33	49.99	72.25	51.70	48.10
$\sigma$	D <sub>-5</sub>	11.47	8.93	15.16	9.59	12.18	17.48	10.12	16.55
	D <sub>-4</sub>	11.88	8.87	17.14	8.74	12.73	22.73	9.71	17.42
	D <sub>-3</sub>	14.11	9.53	15.13	9.56	16.03	25.03	6.13	17.89
	D <sub>-2</sub>	14.00	9.77	15.18	12.21	14.55	28.35	4.25	16.08
	D <sub>-1</sub>	14.25	9.46	16.25	14.15	14.71	30.47	4.34	15.96
D <sub>-5</sub> to D <sub>-1</sub> mean $\sigma$		13.14	9.31	15.87	10.85	14.04	24.81	6.91	16.78
$\sigma$	D <sub>5</sub>	14.52	14.85	13.12	13.98	8.14	36.34	7.15	16.13
	D <sub>6</sub>	15.64	16.14	14.10	13.54	9.82	28.60	8.17	15.19
	D <sub>7</sub>	15.53	15.47	13.18	14.30	1.82	26.94	8.25	14.10
	D <sub>8</sub>	14.92	16.21	11.46	14.58	14.16	23.47	10.06	12.33
	D <sub>9</sub>	13.27	14.85	9.59	14.46	15.17	20.46	10.05	11.36
D <sub>5</sub> to D <sub>9</sub> mean $\sigma$		14.78	15.50	12.29	14.17	11.82	27.16	8.74	13.82

## APPENDIX Ca

(Continued)

Date		1/1/67	11/24/67	12/31/67	2/10/68	3/14/68	12/3/68	12/25/68	3/12/69
$\bar{\phi}$	D <sub>-5</sub>	41.33	51.33	58.58	42.25	48.33	56.33	46.92	61.00
	D <sub>-4</sub>	44.58	51.08	59.92	41.83	47.08	56.92	48.58	61.17
	D <sub>-3</sub>	43.92	50.75	61.42	41.50	48.08	49.75	48.92	61.92
	D <sub>-2</sub>	41.17	51.08	61.25	41.67	48.58	43.67	46.92	63.25
	D <sub>-1</sub>	43.83	50.58	60.67	41.50	47.58	46.17	48.92	61.58
D <sub>-5</sub> thru D <sub>-1</sub> mean $\bar{\phi}$		42.97	50.96	60.37	41.75	47.93	50.57	48.05	61.78
$\bar{\phi}$	D <sub>5</sub>	47.83	49.75	60.83	41.33	52.83	41.50	47.33	63.83
	D <sub>6</sub>	47.83	49.58	70.80	43.00	53.33	42.83	44.08	62.83
	D <sub>7</sub>	47.92	49.67	69.12	43.42	53.58	50.83	50.33	65.08
	D <sub>8</sub>	47.75	47.58	68.00	44.25	53.50	48.08	42.83	63.42
	D <sub>9</sub>	48.67	50.33	72.60	44.33	53.08	50.08	41.82	64.67
D <sub>5</sub> → D <sub>9</sub> mean $\bar{\phi}$		48.00	49.38	68.27	43.27	53.26	46.66	45.28	63.97
$\sigma$	D <sub>-5</sub>	9.53	13.41	12.63	3.37	8.71	25.82	16.62	24.16
	D <sub>-4</sub>	10.31	14.53	11.04	3.78	8.80	28.26	16.29	22.25
	D <sub>-3</sub>	10.44	14.04	10.10	3.50	6.45	24.95	16.08	21.03
	D <sub>-2</sub>	8.86	15.00	11.72	3.97	6.63	19.47	16.85	20.70
	D <sub>-1</sub>	9.20	14.81	16.03	3.75	4.86	23.14	15.88	20.44
D <sub>-5</sub> → D <sub>-1</sub> mean		9.67	14.36	12.30	3.67	7.09	24.33	16.34	21.72
$\sigma$	D <sub>5</sub>	12.35	12.15	15.73	10.15	6.27	13.33	19.15	16.07
	D <sub>6</sub>	13.51	9.94	23.46	10.45	6.82	14.55	18.92	12.75
	D <sub>7</sub>	13.77	10.27	32.87	10.68	7.42	19.90	18.23	10.23
	D <sub>8</sub>	15.39	9.86	33.62	11.19	6.70	17.64	16.50	11.90
	D <sub>9</sub>	14.19	10.48	38.92	9.80	5.77	16.88	10.59	12.04
D <sub>5</sub> → D <sub>1</sub> mean $\sigma$		13.84	10.54	28.92	10.45	6.60	16.46	16.68	12.60

## APPENDIX Cb

Same as Ca except values surround key geomagnetic dates when the polar vortex flow is stable.

Date	11/23/64	11/20/64	1/1/65	2/7/67	1/17/69	2/27/69	
$\bar{\phi}$	D <sub>-5</sub>	48.00	52.67	50.83	52.33	41.67	58.83
	D <sub>-4</sub>	48.25	53.50	50.58	51.75	42.67	53.25
	D <sub>-3</sub>	49.75	52.67	50.33	51.83	42.42	53.75
	D <sub>-2</sub>	49.83	51.50	49.83	51.08	43.92	52.58
	D <sub>-1</sub>	49.42	52.67	48.58	50.00	44.50	54.75
D <sub>-5</sub> → D <sub>-1</sub> mean $\bar{\phi}$	49.05	52.40	50.03	51.40	43.03	54.63	
$\bar{\phi}$	D <sub>5</sub>	48.67	50.92	48.42	52.58	41.33	57.17
	D <sub>6</sub>	49.42	50.83	48.83	52.00	42.75	58.25
	D <sub>7</sub>	48.50	50.58	49.17	51.83	44.83	60.00
	D <sub>8</sub>	48.00	50.33	48.83	51.75	45.25	61.00
	D <sub>9</sub>	49.25	49.83	48.92	51.83	43.00	61.17
D <sub>5</sub> → D <sub>9</sub> mean $\bar{\phi}$	48.77	50.50	48.83	52.00	43.43	59.52	
$\sigma$	D <sub>-5</sub>	10.14	13.00	15.85	16.73	10.99	9.50
	D <sub>-4</sub>	10.99	14.76	16.08	17.03	13.01	14.17
	D <sub>-3</sub>	12.16	14.79	16.10	16.39	15.07	10.31
	D <sub>-2</sub>	13.09	15.77	16.45	15.86	13.55	10.68
	D <sub>-1</sub>	14.19	15.15	15.54	15.05	12.60	9.83
D <sub>-5</sub> → D <sub>-1</sub> mean $\sigma$	12.11	14.69	16.00	16.21	13.04	10.90	
$\sigma$	D <sub>5</sub>	11.30	14.49	15.10	9.97	7.17	22.25
	D <sub>6</sub>	10.27	15.85	17.21	9.40	7.84	22.25
	D <sub>7</sub>	10.11	16.08	19.36	8.80	13.30	23.89
	D <sub>8</sub>	8.55	16.10	18.37	10.26	15.16	24.16
	D <sub>9</sub>	7.96	16.45	20.20	1.59	17.59	22.25
D <sub>5</sub> → D <sub>9</sub> mean $\sigma$	9.64	15.79	18.05	10.00	12.21	22.96	

## Appendix A

1. Assume a mean temperature of 218°K [-55°C] in the 30 mb-10 mb layer.
2. Given the formula from the Smithsonian Tables:

$$\Delta\phi = 67.442 (273.16 + t'_{mv}) \log_{10} \frac{P_1}{P_2}$$

where:  $\Delta\phi$  = thickness of the layer (gpm)

$t'_{mv}$  = mean adjusted virtual temperature of the layer  
(°C)

$P_1$  = pressure at the base of the layer

$P_2$  = pressure at the top of the layer

3. Using this formula with the values given in (1.) above

$$\Delta\phi = 7020 \text{ gpm}$$

4. If we increase the thickness of this layer by 320 gpm and reapply the equation in (2.),

$$t'_{mv} = -45^\circ\text{C}$$

5. Therefore, corresponding to an increase of 320 gpm in the 30 mb-10 mb layer, the mean virtual temperature must increase by 10°C.
6. From the text, we had assumed that the area of the latitude band in which auroral energy is absorbed is  $5.6 \times 10^{16} \text{ cm}^2$ .
7. The mass of air in the 30 mb-10 mb layer over this band is  $(20 \text{ g cm}^{-2}) (5.6 \times 10^{16} \text{ cm}^2) = 1.1 \times 10^{18} \text{ g}$ .
8. Given the specific heat of air  $c_p = 10 \text{ erg g}^{-1} \text{ }^\circ\text{K}^{-1}$ .
9. The energy required to bring about this observed warming = (total mass to be heated) (specific heat of the mass) (change in temperature

required), or from (7.), (8.), and (5.) above. Energy required =  
 $(1.1 \times 10^{18} \text{g}) (10^6 \text{erg g}^{-1} \text{ } ^\circ\text{K}^{-1}) (10^\circ\text{K}) = 1.1 \times 10^{25} \text{erg}.$

10. From Matsushita and Campbell, assume that the energy of an auroral absorption is  $10^{18} \text{erg sec}^{-1}$ .
11. Assume that this strong absorption lasts  $\sim 3$  hours or  $10^4$  sec.
12. Then the total energy involved in the aurora is

$$(10^{18} \text{erg sec}^{-1}) (10^4 \text{sec}) = 10^{22} \text{ erg}.$$

13. Comparing the results from (9.) and (12.), note that the energy involved in an aurora is much less than is required to produce the noted heating.

## Appendix B

Assume a four degree increase in mean latitude of the 30,640m contour at 10 mb, and assume that this is brought about by the 10°K warming in the 30 mb-10 mb layer noted in appendix A.

Differentiating Poisson's equation and holding  $d\theta = 0$  where  $P = 20$  mb,  $T = 223^\circ\text{K}$ , let  $dT = + 10^\circ\text{K}$

$$d\theta = dT \left( \frac{1000}{P} \right)^K + = KT(1000)^K P^{-K-1} dp$$

$$\text{then } dp = 3.1 \text{ mb}$$

Using the hydrostatic approximation, this corresponds to a change of about 1070 gpm.

Therefore a parcel of air which sinks adiabatically from the 20 mb level,  $T = 223^\circ\text{K}$ , and warms  $10^\circ\text{K}$  must experience a change in geopotential of  $\sim 1070$  gpm.

If this change in geopotential is experienced over a period of nine days ( $7.78 \times 10^5 \text{sec}$ ), then the mean vertical motion which accounts for this warming is about  $-.14 \text{ cm sec}^{-1}$ .



